THE JOURNAL OF COMPARATIVE NEUROLOGY 412:319–341 (1999)

Broca's Region Revisited: Cytoarchitecture and Intersubject Variability

KATRIN AMUNTS,[1]* AXEL SCHLEICHER,[1] ULI BÜRGEL,[1] HARTMUT MOHLBERG,[1] HARRY B.M. UYLINGS,[2] AND KARL ZILLES[1,3]

[1]C. and O. Vogt Institute for Brain Research, Heinrich Heine University, D-40001 Düsseldorf, Germany

[2]Netherlands Institute for Brain Research, 1105 AZ Amsterdam, The Netherlands

[3]Institute of Medicine, Research Center Jülich, D-52425 Jülich, Germany

ABSTRACT

The sizes of Brodmann's areas 44 and 45 (Broca's speech region) and their extent in relation to macroscopic landmarks and surrounding areas differ considerably among the available cytoarchitectonic maps. Such variability may be due to intersubject differences in anatomy, observer-dependent discrepancies in cytoarchitectonic mapping, or both. Because a reliable definition of cytoarchitectonic borders is important for interpreting functional imaging data, we mapped areas 44 and 45 by means of an observer-independent technique. In 10 human brains, the laminar distributions of cell densities were measured vertical to the cortical surface in serial coronal sections stained for perikarya. Thousands of density profiles were obtained. Cytoarchitectonic borders were defined as statistically significant changes in laminar patterns. The analysis of the three-dimensional reconstructed brains and the two areas showed that cytoarchitectonic borders did not consistently coincide with sulcal contours. Therefore, macroscopic features are not reliable landmarks of cytoarchitectonic borders. Intersubject variability in the cytoarchitecture of areas 44 and 45 was significantly greater than cytoarchitectonic differences between these areas in individual brains. Although the volumes of area 44 differed across subjects by up to a factor of 10, area 44 but not area 45 was left-over-right asymmetrical in all brains. All five male but only three of five female brains had significantly higher cell densities on the left than on the right side. Such hemispheric and gender differences were not detected in area 45. These morphologic asymmetries of area 44 provide a putative correlate of the functional lateralization of speech production. J. Comp. Neurol. 412:319–341, 1999.

Indexing terms: brain mapping; anterior speech region; asymmetry; gender differences; volume; cell density

The cytoarchitectonic areas 44 and 45 are located at the inferior frontal gyrus and occupy the partes opercularis and triangularis (Brodmann, 1909). It is widely accepted that both areas constitute the anatomical correlates of Broca's region (Aboitiz and Garcia, 1997). The analysis of Broca's region (Broca, 1861) is of long-standing interest because fluent speech is most likely to be affected by lesions of the left inferior frontal gyrus, where Broca's region is located (Brown, 1972; McGlone, 1977; Mohr et al., 1978; Levine and Mohr, 1979; Damasio, 1992; Buckner et al., 1996; Caplan et al., 1996). This region also seems to participate in stuttering (Fox et al., 1996; Braun et al., 1997). It has been demonstrated that the homologous region in the right, nondominant hemisphere may be involved in prosodic aspects of speech (Botez and Wertheim, 1959) and in the detection of syntactic errors (Bradvik et al., 1991; Nichelli et al., 1995). More detailed functional aspects of Broca's region were examined by investigators using different verbal tasks and positron emission tomography (Ingvar and Schwartz, 1974; Roland et al., 1985; Petersen et al., 1988; Mazziotta and Metter,

Grant sponsor: Deutsche Forschungsgemeinschaft; Grant number: SFB 194/A6; Grant sponsor: Biomed; Grant number: BMH4-CT95–0789; Grant sponsor: Biotech; Grant number: Bio-CT 96–0/77.

*Correspondence to: Katrin Amunts, C. and O. Vogt Institute for Brain Research, Heinrich Heine University, Postfach 101007, D-40001 Düsseldorf, Germany. E-mail: katrin@hirn.uni-duesseldorf.de

Received 8 September 1998; Revised 27 January 1999; Accepted 10 May 1999

1988; Demonet et al., 1992; Zatorre et al., 1992; Mazoyer et al., 1993; Petrides et al., 1993; Frackowiak, 1994; Nathaniel-James et al., 1997). Functional magnetic resonance imaging (McCarthy et al., 1993; Desmond et al., 1995; Binder et al., 1996; Hertz-Pannier et al., 1997; Indefrey et al., 1998), magnetoencephalography (Martin et al., 1993), and electrical stimulation (Penfield and Rasmussen, 1949; Ojeman, 1991) have also been employed. Activation was usually elicited in the left inferior frontal gyrus, but in some cases it was also found in the homologous region of the right hemisphere (Roland et al., 1985; Mazoyer et al., 1993; Just et al., 1996). Gender-specific lateralization has recently been discovered: activation in males occurred only in the left inferior frontal gyrus but on both sides in females (Shaywitz et al., 1995). Unfortunately, these researchers did not substantiate this finding statistically. Gender differences in other anatomical measures of asymmetry (e.g., surface or volume) have been described for several regions including the Sylvian fissure, the planum parietale and corpus callosum (Berrebi et al., 1988; Kertesz et al., 1990; Habib et al., 1991; Witelson and Kigar, 1992; Jäncke et al., 1994; Steinmetz et al., 1995; Ide et al., 1996), and Broca's region (Uylings et al., 1999). Previous cytoarchitectonic studies did not report on differences between the areas of the anterior speech regions of either side of normal brains (Brodmann, 1909; Economo and Koskinas, 1925). Therefore, it is still a matter of discussion whether or not cytoarchitectonic features are associated with functional lateralization of speech (Galaburda, 1980; Scheibel et al., 1985; Simonds and Scheibel, 1989; Jacobs et al., 1993a; Hayes and Lewis, 1995; Hayes and Lewis, 1996).

The early cytoarchitectonic analyses of both areas were, to a large extent, restricted to qualitative descriptions of cell morphology and laminar patterns (Kononova, 1949). In some studies, qualitative aspects (Stengel, 1930; Riegele, 1931; Strasburger, 1938) were supplemented by quantitative measurements (Economo and Koskinas, 1925; Kononova, 1935; Rabinowicz, 1967). The classic descriptions differ considerably with respect to the extent, location, and sizes of areas 44 and 45 (Fig. 1). Architectonic features were reported to be highly variable among subjects (Kononova, 1935). Variability also concerns, e.g., the size of area 44 on the free surface of the pars opercularis (compare the maps of Brodmann and Economo–Koskinas with those of the Russian school), the location of area 45 with respect to the horizontal branch of the Sylvian fissure (compare the maps of Economo–Koskinas with those of Brodmann and the Russian school), and the sulcal patterns of the pars triangularis. In addition, the surrounding areas also differ between maps. Whereas Brodmann found that areas 46 and 9 are located in the dorsal neighborhood of areas 44 and 45, the Russian school reported that areas 8 and 9 but not area 46 constitute the neighborhood of areas of 44 and 45. It has to be considered that the maps themselves present only the superficially exposed part of the cortical surface. A much larger part of the surface, however, is buried in the sulci (Falzi et al., 1982; Zilles et al., 1988).

The precise functional differences between both areas are still not known. In some verbal tasks, clusters of functional activation were scattered over the entire extent of Broca's region (Demonet et al., 1992; Hinke et al., 1993; Mazoyer et al., 1993; Hirano et al., 1996), but, in other tasks, activation occurred only in parts, i.e., in locations corresponding approximately to area 44, or to areas 44 and 6, or to area 45 (Sergent et al., 1992; Fox et al., 1996; Herholz et al., 1996; Paulesu et al., 1996; Kim et al., 1997). For some critical comments, see Poeppel (1996a,b).

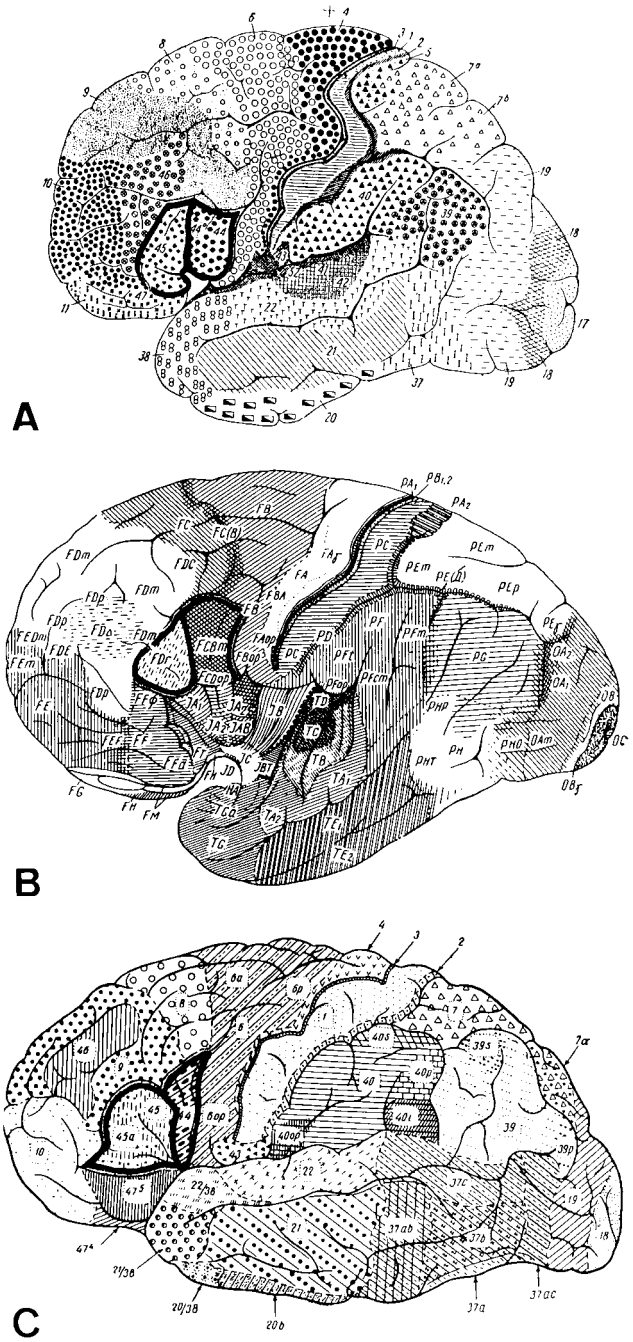

Fig. 1. Cytoarchitectonic maps of the lateral surface of human brain adapted from (**A**) Brodmann (1909), (**B**) Economo and Koskinas (1925), and (**C**) the Russian school (Sarkisov et al., 1949). Cytoarchitectonic areas are marked by different hatch marks and are classified according to Brodmann's nomenclature by arabic numerals (A,C) or according to that of Economo and Koskinas by letters and numerals (B). Note the differences in sulcal patterns and in the shapes and extents of areas 44 and 45. FCBm of Economo and Koskinas corresponds to Brodmann's area 44, FDΓ corresponds to Brodmann's area 45. The locations of areas 44 and 45 in each map are indicated by bold lines.

TABLE 1. Brains Used in the Present Study

Case	Age (years)	Gender[1]	Cause of death	Postmortem delay (hours)	Brain weight (g) before fixation	Fixation
1	79	f	Carcinoma of the bladder	24	1,350	Bodian
2	55	m	Rectal carcinoma	24	1,270	Formalin
3	68	m	Vascular disease	16	1,360	Formalin
4	75	m	Acute glomerulonephritis	24	1,349	Formalin
5	59	f	Cardiorespiratory insufficiency	24	1,142	Formalin
6	54	m	Cardiac infarction	8	1,757	Formalin
7	37	m	Cardiac arrest	24	1,437	Formalin
8	72	f	Renal arrest	12	1,216	Formalin
9	79	f	Cardiorespiratory insufficiency	16	1,110	Bodian
10	85	f	Mesenteric infarction	14	1,046	Bodian

[1]f, female; m, male.

In addition to structural variability, the previous methods for defining cytoarchitectonic borders may have contributed to interobserver differences. It is well known that the definition of cytoarchitectonic borders depends to a large extent on the experience and abilities of the investigator to recognize patterns. This methodological aspect must be considered when critically evaluating previous studies (Bonin and Bailey, 1961). Because local changes in the laminar distribution of cell packing densities have long been a major criterion for defining areal borders in conventional cytoarchitectonic studies (Brodmann, 1909), we have applied a new quantitative and observer-independent approach to compare these densities. The laminar distribution of cell densities was measured with an automated microscopic scanning procedure using an image analysis system (Schleicher and Zilles, 1990). The resulting gray level index (GLI) is a reliable measure of cell packing density in the cortex (Wree et al., 1982). The approach can be used to quantitatively describe cytoarchitecture by measuring the GLI distribution along a vertical trajectory from the cortical surface to the white matter (Schleicher and Zilles, 1990). Statistically significant changes in the laminar distribution of the GLI can be detected at the transition between two cytoarchitectonic areas but not within an homogeneous area (Schleicher et al., 1995, 1998). A procedure based on the detection of such changes in GLI has been shown to be sensitive for interhemispheric, ontogenetic, and areal differences (Zilles et al., 1986b; Schlaug et al., 1995b; Amunts et al., 1996, 1997; Geyer et al., 1996, 1997). Thus, this procedure avoids observer-dependent influences in defining areal borders and makes possible the statistical testing for significant changes in cytoarchitectonic organization.

The aims of the present study were to (1) determine the positions and extents of areas 44 and 45 in the left and right hemispheres in serial histologic sections through 10 human brains by applying an observer-independent procedure for the definition of cytoarchitectonic borders, (2) examine whether there are any areal-, side-, and gender-dependent differences in the cytoarchitecture of the two areas, (3) test whether it is possible to predict the precise location of cytoarchitectonic borders on the basis of sulcal features, and (4) analyze intersubject variability in the extent and cytoarchitecture of both areas.

MATERIALS AND METHODS

Subjects

Ten human brains (five male, five female; age range = 37–85 years) were studied (Table 1). Subjects were obtained by body donor programs of the Anatomical Institute of the University of Düsseldorf or from collaboration between the Anatomical Institute and departments of pathology in accordance with legal requirements. The autopsies were performed within 8–24 hours after death. Case 3 came from a subject with transitory motor disturbances (not affecting speech); all other subjects had no indications of neurologic or psychiatric diseases in clinical records. Handedness and language dominance of the subjects were not known. Considering an incidence of about 95% of left-sided language dominance (Branche et al., 1964), it is likely that most of our cases were dominant for the left side.

Histology

The brains were fixed in either in 4% buffered formalin (pH 7.4) or a mixture of formalin, glacial acetic acid, and ethanol (Bodian mixture). The whole paraffin-embedded brains were serially sectioned in the coronal plane; 6,000–7,500 sections (20 µm thick) per brain were obtained. Each 15th section was mounted on a glass slide and silver stained for cell bodies (Merker, 1983). Each 60th section of the total number was used for analysis.

Quantitative cytoarchitecture

Regions of interest (ROIs) containing Broca's region were selected for quantitative cytoarchitectonic analysis. The GLI (Zilles et al., 1986; Schleicher and Zilles, 1990) is a measure of the volume fraction of somata per volume of unit brain tissue. It is highly correlated with cell density (Wree et al., 1982). The GLI was determined by using an image analyzer (KS400, Zeiss) connected to a microscope with a motor stage for automated scanning and focusing. Digitized high-resolution GLI images of the ROIs were obtained and printed (Fig. 2A). The GLI of each pixel of these images represents the volume fraction occupied by cell bodies in a square measuring field of 32×32 µm.

Laminar changes in cortical cell density were registered as GLI profiles along trajectories running parallel to the orientation of cell columns, i.e., vertical to the cortical surface, from the border between layers I and II to the border between the cortex and white matter. The profiles covered the cortex in the ROIs at equidistant intervals of approximately 128 µm (Fig. 2A). Positions of profiles were numbered consecutively from 1 to n, where n was the number of profiles per ROI.

Each GLI profile (see Fig. 3, Table 2) was characterized by a set of 10 features (feature vector). Features were based on central moments (Dixon et al., 1988), as follows: the mean GLI value (meany.o), the center of gravity in the x-direction (meanx.o), the standard deviation (sd.o), the skewness (skew.o), the kurtosis (kurt.o), and the analogous

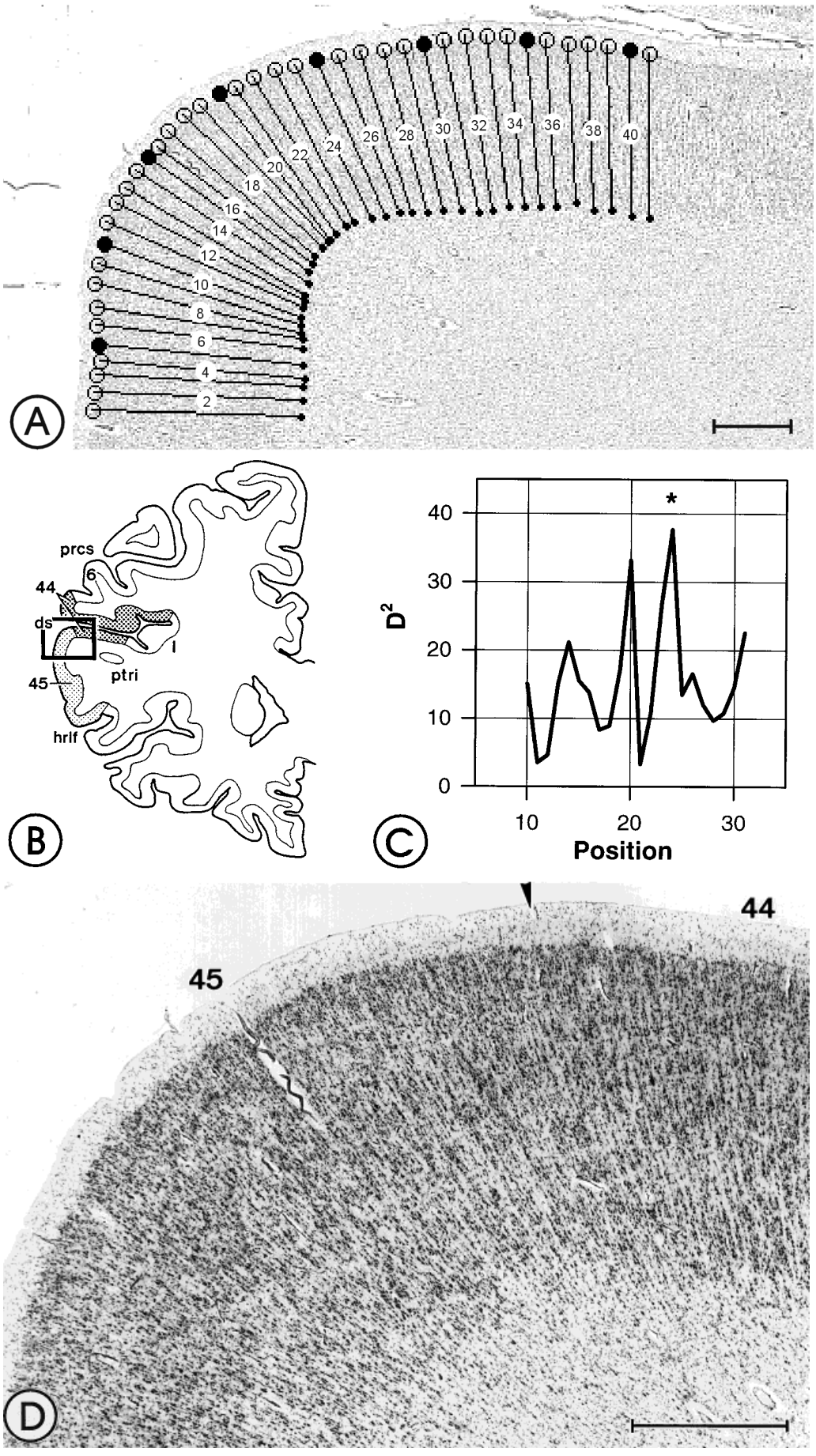

Figure 2

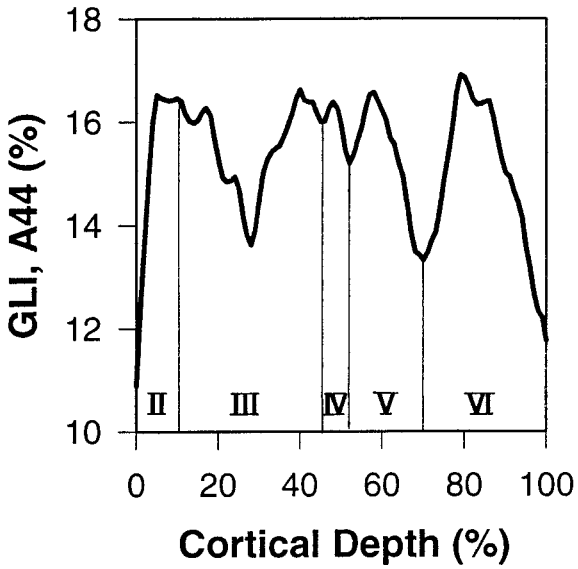

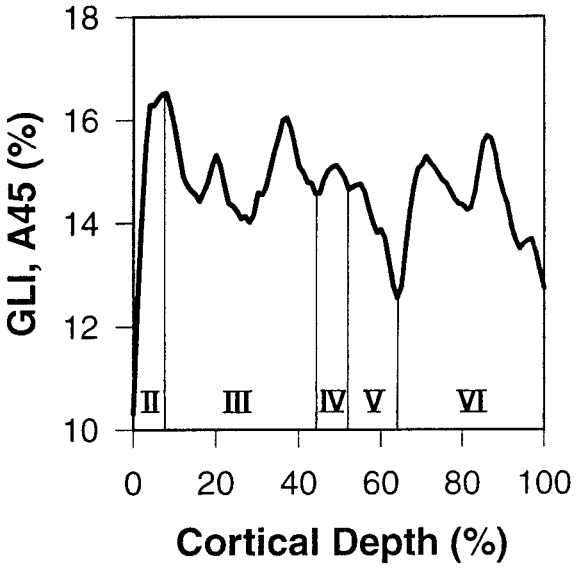

Fig. 3. Mean cell density profiles (ordinate, gray level index; GLI, in %) for areas 44 (left) and 45 (right) of case 6 showing laminar changes from the layer I/II border (abscissa, 0%) to the white matter (abscissa, 100%). Profiles were obtained from the section shown in Figure 2. Ten individual profiles were averaged for each area: profiles at positions 15–24 for area 45 and at positions 25–34 for area 44 (see Fig. 2). Shape differences between profiles from areas 44 and 45 were significant ($P < 0.05$). The corresponding mean values of the 10 shape-describing features of the profiles of areas 44 and 45 are presented in Table 2. Roman numerals indicate different cortical layers.

parameters for the first derivative of each profile (meany.d, meanx.d, sd.d, skew.d, kurt.d). These features are to a certain degree abstract parameters that were derived from the mathematical analysis of frequency distributions. They allowed a quantitative analysis of the shapes of profiles and of the differences between neighboring profiles (Schleicher et al., 1995, 1998). Some features, however, can be interpreted directly in terms of cytoarchitecture: the mean GLI increases with increasing density of cell bodies. The feature meanx.o will be smaller than 50% if the supragranular layers have a higher GLI than the infragranular layers; and vice versa, if the infragranular layers show more densely packed cell bodies than the supragranular layers, the meanx.o will be shifted to a value greater than 50%.

TABLE 2. Values of the 10 Features (Feature Vector) ± S.D. Corresponding to the Two Mean Cell Density Profiles From Figure 3[1]

	Area 44	Area 45
meany.o (%)	15.27 ± 0.29	14.45 ± 0.55
meanx.o (%)	49.49 ± 0.939	49.70 ± 1.076
sd.o (%)	28.85 ± 0.362	28.91 ± 0.525
skew.o	0.010 ± 0.050	0.017 ± 0.066
kurt.o	−1.198 ± 0.033	−1.199 ± 0.026
meany.d	1.572 ± 0.209	1.480 ± 0.148
meanx.d	47.59 ± 3.424	47.14 ± 2.931
sd.d	30.34 ± 1.826	30.00 ± 1.242
skew.d	−0.002 ± 0.174	−0.003 ± 0.146
kurt.d	−1.246 ± 0.191	−1.222 ± 0.061

[1]meany.o, mean gray level index; meanx.o, center of gravity in x-direction; sd.o, standard deviation; skew.o, skewness; kurt.o, kurtosis; analogous parameters for the first derivative of each profile (meany.d, meanx.d; sd.d, skew.d; kurt.d).

Fig. 2. An example of the definition of cytoarchitectonic borders in case 6. **A:** Digitized image with a cortical region containing parts of areas 44 and 45. The gray value of each pixel in this image indicates the volume fraction of cell bodies, which is a good estimate of cell packing density: a high gray level index (GLI) is represented by a dark pixel, a low GLI by a correspondingly brighter pixel. The cortex was covered with vertical lines running from the border between layers I and II to the cortex/white matter border. Along each line, a GLI profile was measured. In this case, the positions of the profiles were numbered from 1 to 41, with equidistant intervals of approximately 128 µm. **B:** Location of the image shown in A in the corresponding section from the left hemisphere. **C:** The Mahalanobis distance (D^2) versus the position of the profile (distance function). Each D^2 value was calculated for the distance between two neighboring blocks of profiles, with 10 profiles per block. A significant D^2 was found at position 24 (asterisk). This peak marked the border between areas 44 and 45. The smaller peak at position 20 was not accepted as a border different from that at position 24 because the distance between both peaks at positions 20 and 24 is below the resolution given by the block size of 10 profiles. **D:** Corresponding micrograph with the border between areas 44 and 45 (arrowhead corresponds to position 24). prcs, precentral sulcus; ptri, pars triangularis; ds, diagonal sulcus; hrlf, horizontal ramus of the lateral fissure; I, insula; 6, Brodmann's area 6. Scale bars = 1 mm.

Observer-independent definition of borders

The observer-independent definition of borders between cortical areas is based on the assumption that feature vectors of cell density profiles from two different cytoarchitectonic areas differ significantly, whereas profiles in one and the same area are not significantly different. The differences between profiles were evaluated by using multivariate statistics. They were expressed as the Mahalanobis distances (D^2) between two adjacent blocks of profiles, each of which consisted of 10 neighboring profiles. The width of a block was approximately 1.28 mm. After the calculation of D^2 for two adjacent blocks of profiles, both blocks were shifted simultaneously by ~128 µm (i.e., one profile) to the next possible location. In this manner, D^2 was calculated continuously for all sequential positions of all possible blocks of profiles in the region studied (Fig. 2C). For example, D^2 at position 10 was calculated between the first block containing the profiles 1–10 and the second

block containing the profiles 11–20 (Fig. 2C). D^2 at position 11 corresponded to the distance between the block with profiles 2–11 and the block with profiles 12–21.

D^2 increases with increasing differences in the shapes of the profiles of two neighboring blocks. A subsequent Hotelling T^2 test was applied for testing the significance of each D^2 value. Borders between areas were defined only at those positions that showed significant distances at a level of $\alpha = 5\%$. In the case of multiple significant maxima within a distance of 1.28 mm, i.e., within the width of one block, only the highest maximum was accepted and the smaller maxima were rejected (Schleicher et al., 1998; compare the peaks at positions 20 and 24 in Fig. 2C,D). Thus, the spatial resolution in the present study is 1.28 mm.

Interareal, interhemispheric, and gender comparisons of cytoarchitectonic parameters and volumes

After defining the borders of areas 44 and 45, interareal, interhemispheric, and gender differences in cell density were investigated. Three ROIs were sampled per area and hemisphere. For selecting the ROIs, all sections in which areas 44 and 45 occurred were subdivided into three samples, equal in numbers of sections. From each sample, one section was selected randomly for quantitative analysis. Eight equidistant GLI profiles were measured per section and area. The profiles were normalized to a cortical depth of 100% to compare regions of different cortical thicknesses. One mean profile for each area and hemisphere was calculated by averaging 24 GLI profiles (3 sections $\times$ 8 profiles). Thus, a total of 40 mean profiles (10 brains $\times$ 2 hemispheres $\times$ 2 areas) was obtained for interareal and interhemispheric comparisons. Differences in cytoarchitecture between the hemispheres of each brain and between areas were analyzed by calculating the Mahalanobis distances between the profiles and applying the Hotelling's T^2 test ($\alpha = 0.05$).

The mean GLI, collapsed over all layers (overall cell density), was calculated for a cortical area in each brain and hemisphere. Side and gender differences were tested by analysis of variance (ANOVA). The statistical design of this two-way ANOVA was as follows: the two factors were side of hemisphere (left, right) and gender (male, female); the blocking factor was subject. The level of significance was Bonferroni-corrected from 0.05 to 0.025 for multiple comparisons (male and female).

Left–right differences in overall cell density were analyzed further by using the asymmetry coefficient (AC, %) as described previously (Uylings et al., 1984; Galaburda et al., 1987). Differences were calculated for areas 44 and 45 according to the formula

$$AC = 100\% \times (GLI_L - GLI_R)/[(GLI_L + GLI_R)/2] \quad (1)$$

where GLI_L and GLI_R are the mean cell densities for the left and right hemispheres, respectively.

Relative layer thicknesses were calculated in areas 44 and 45 to estimate the proportion of each layer in relation to cortical depth as a whole. The thicknesses of the cortical layers II–VI were measured after identification under the microscope. Layer IV of area 44 appeared to be invaded by pyramidal cells from neighboring layers III and V. Its thickness was defined by the presence of granular cells. Single pyramidal cells from layers III and V were disregarded. Differences in relative layer thickness were analyzed with ANOVA. The statistical design of the three-way ANOVA was as follows: the three factors were area (44, 45), side of hemisphere (left, right), and layer (II, III, IV, V, VI); the blocking factor was subject.

The volumes of areas 44 and 45 were measured according to Cavalieri's principle (Uylings et al., 1986). In dependence on the extent of each area, 7–11 sections were analyzed per brain and hemisphere to calculate the volumes. Left–right comparisons of volumes were performed by a paired (left vs. right hemisphere) t-test with Bonferroni correction for multiple tests ($P < 0.025$). Asymmetry coefficients for volumes (AC_{vol}) were calculated similar to equation (1). Statistical analysis was performed by using the software package SYSTAT.

Analysis of intersubject variability in cytoarchitecture

Intersubject variability in cytoarchitecture was analyzed by comparing intraareal (intersubject) differences in profiles obtained from one and the same area of different brains, with interareal (intrasubject) differences between profiles from area 44 and profiles from area 45 of each single brain. Mean D^2 for intraareal and interareal differences were thus calculated. The number of possible intraareal differences for all brains was 45. This number was calculated as $(9 \times 10)/2$ (each of the 10 brains was compared with the 9 remaining brains; this value was then divided by 2 because the results are identical when brain A is compared with B or, vice versa, brain B is compared with A). The number of possible interareal differences was 10 (one comparison between areas 44 and 45 per brain). There was no significant left–right asymmetry in interareal differences; thus, profiles of the left and the right hemispheres were collapsed for examining interareal differences. The significance of D^2 between intraareal (intersubject) and interareal differences was tested by a Kruskal-Wallis one-way rank analysis ($\alpha = 0.05$). This procedure answers the question of whether intersubject variability in cytoarchitecture of areas 44 and 45 is greater or lower than interareal differences in each brain.

Cytoarchitectonic identity of areas defined by the present approach

The cytoarchitectonic identity of the areas determined by the present quantitative approach was established by comparing the present findings with the descriptions and micrographs published by Economo and Koskinas (1925). Their FCBm corresponds to Brodmann's and our area 44, and their FDΓ corresponds to Brodmann's and our area 45 (Fig. 1). The description by Economo and Koskinas does not differ essentially from that of Kononova (1949) who used Brodmann's nomenclature except for the slight modification of introducing subarea 45a at the rostral border of area 45 (Fig. 1). FCBm (area 44) is a dysgranular area between the agranular frontal (premotor cortex) and the granular prefrontal cortex. The index m indicates that this area has conspicuously large pyramidal cells in deep layer III (magnopyramidal). The height of deep layer III nerve cell bodies is 60–70 μm, and the width is 25 μm. The borders of layer IV to layers III and V undulate. The cortex of FCBm is not sharply delineable from the underlying white matter. FCBm contains clearly visible cell columns and a distinct but thin layer II. Layer V can be subdivided

into an upper sublayer with more densely packed cells and a lower sublayer with fewer cells. FDΓ (area 45) has a thinner cortex than FCBm but has distinct horizontal layering and prominent cell columns in addition to large pyramidal cells in deep layer III (Economo and Koskinas, 1925). The identification of the neighboring areas (6, 8, 9, 10, 46, 47, insula) was also based on criteria provided by Economo and Koskinas. For identifying areas 9 and 46, the results of a recent study by Rajkowska and Goldman-Rakic were also considered (1995a,b).

In conclusion, the cytoarchitecture of our areas 44 and 45 closely fits that of previous descriptions of these areas by Economo and Koskinas (1925) and Kononova (1949). Brodmann's (1909) description is too cursory for sufficiently detailed comparison. More recent cytoarchitectonic criteria of areas 9 and 46 were also recognizable in our sections (Rajkowska and Goldman-Rakic, 1995a,b).

Superimposition of areas 44 and 45 on the surface of the brain

The borders of areas 44 and 45 were displayed on three-dimensional (3-D) reconstructions of the individual brains. This required several steps. High-resolution magnetic resonance (MR) sequences of the postmortem brains were obtained after fixation but prior to embedding, sectioning, and staining, as previously described (Roland and Zilles, 1994; Zilles et al., 1995; Amunts et al., 1996; Geyer et al., 1996). MR imaging was performed with a Siemens 1.5 T magnet (Erlangen, Germany) with a T1-weighted FLASH sequence (flip angle = 40°, repetition time = 40 msec, echo time = 5 msec for each image). Each volume consisted of 128 sagittal sections that covered the entire brain. Spatial resolution was $1 \times 1 \times 1.17$ mm (Steinmetz et al., 1990). Each voxel had a resolution of eight bits corresponding to 256 gray values. The brain volumes were spatially transformed into the standard format of the human brain atlas (Roland and Zilles, 1994) and oriented in the plane determined by the anterior–posterior commissures, i.e., the AC–PC plane (Talairach and Tournoux, 1988).

Images of histologic silver-stained sections were digitized with a CCD camera. To reconstruct the histologic volume, each brain was represented by three data sets: (1) the histologic data set with high contrast but with distortions caused by histologic techniques, (2) a photo-data set with low contrast (resulting from the unstained surface of the paraffin block) showing the histologic section before sectioning and a reference system to establish the 3-D integrity of the histologic volume, and (3) and the MR-data set obtained prior to embedding with improved contrast but at a slightly different orientation than the photo-data set (Schormann and Zilles, 1998). The comparison of these three data sets allowed us to correct for deformations and shrinkage inevitably caused by histologic techniques, e.g., embedding, sectioning, and mounting on glass slides. Both linear affine and nonlinear fluid transformations were applied (Schormann et al., 1993, 1995; Schormann and Zilles, 1997, 1998).

The extents of areas 44 and 45 on both sides in the histologic sections were interactively traced into the corresponding MR image by using an image analysis system (KS400, Zeiss). The cytoarchitectonic areas were 3-D reconstructed. The surface rendering of the 3-D reconstructed areas was performed by using the AVS software package (Uniras, Germany).

RESULTS

Identification of areas 44 and 45 and definition of borders

Area 44 was identified on the basis of conspicuously large pyramidal cells in deep layer III and in layer V and by a barely recognizable dysgranular layer IV, which was invaded to different degrees by layer III and V pyramidal cells (Fig. 4A). Area 45 differed essentially from area 44 by the presence of a clearly visible layer IV. Due to the more pronounced layer IV, the horizontal layering of area 45 also appeared more conspicuous than did that of area 44. Layer IV of area 45, however, was less distinct than that in the rostrally adjoining prefrontal cortex, e.g., in areas 10 or 46 (Fig. 4B). These qualitative findings allowed us to identify regions that had been delineated with the observer-independent quantitative procedure as cortical units comparable to Brodmann areas 44 and 45.

The observer-independent approach demonstrated significant differences between the shapes of cell density profiles in areas 44 and 45 after multivariate statistics and a noneuclidean distance function was applied (see section Observer-independent definition of borders). The distance function showed maximal values when the profiles were located at the opposite sides of an areal border. As an example, Figure 3 shows neighboring profiles from the border between areas 44 and 45 in subject 6 (Fig. 2). The laminar distribution pattern of cell bodies, i.e., the feature vectors, differed significantly between areas 44 and 45 ($P < 0.05$; see also Table 2).

This border between areas 44 and 45 was detectable in all 10 brains (Figs. 2, 5, 6). Only in three sections did a significant "border" detected by the automated procedure need to be rejected because of histologic artifacts (tissue defects introduced by the sectioning and mounting procedures). It is readily understandable that such artifacts alter the laminar pattern and will lead to the detection of artificial "borders." However, such artifacts were always easily recognizable and clearly localizable in the distance function curve. Smaller ruptures of the tissue, as shown in Figure 7, did not cause artificial borders.

In addition to the borders between areas 44 and 45, we found other significant borders within each area. These borders subdivided areas 44 and 45 into two or more parts, each of which had an extent of approximately 3–8 mm along the cortical surface (e.g., Fig. 7). These borders were not "artificial," i.e., caused by artifacts. They could be identified on adjacent histologic sections. In some cases, such borders were found at the transition between the crown and the wall of a gyrus (e.g., border within area 44 at position 52 in Fig. 7). Other borders did not coincide with changes in gyral geometry (e.g., border at position 68 in Fig. 7). Because a systematic mapping of all subdivisions in areas 44 and 45 was not within the scope of the present study, further observations will be necessary for an analysis of the significance of these subdivisions and their possible association with functional heterogeneity in Broca's region.

The outer borders of Broca's region (borders to Brodmann's areas 6, 8, 9, 10, 46, 47, and to the insular cortex) were also defined by using the observer-independent procedure (Figs. 6–11). Area 47 is located ventral to areas 44 and 45. However, area 47 does not seem to be homogeneous because it consists of several subareas. These subareas are arranged in a lateroorbital sequence (Kononova, 1935). By

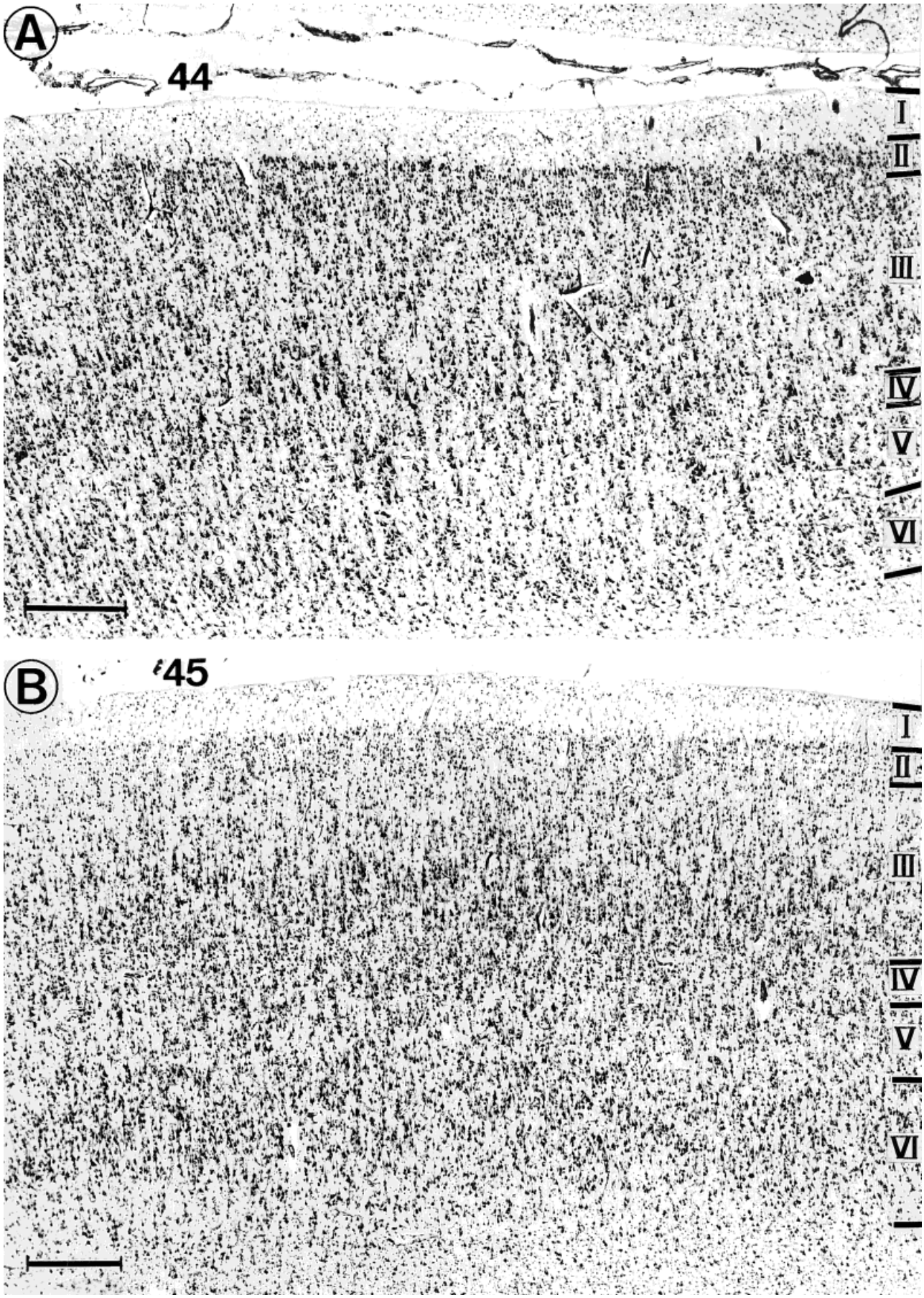

Fig. 4. Photomicrographs of cytoarchitecture of areas 44 (**A**) and 45 (**B**) in coronal, cell body-stained sections. Case 9, left hemisphere. Roman numerals indicate the different cortical layers. Scale bars = 0.5 mm.

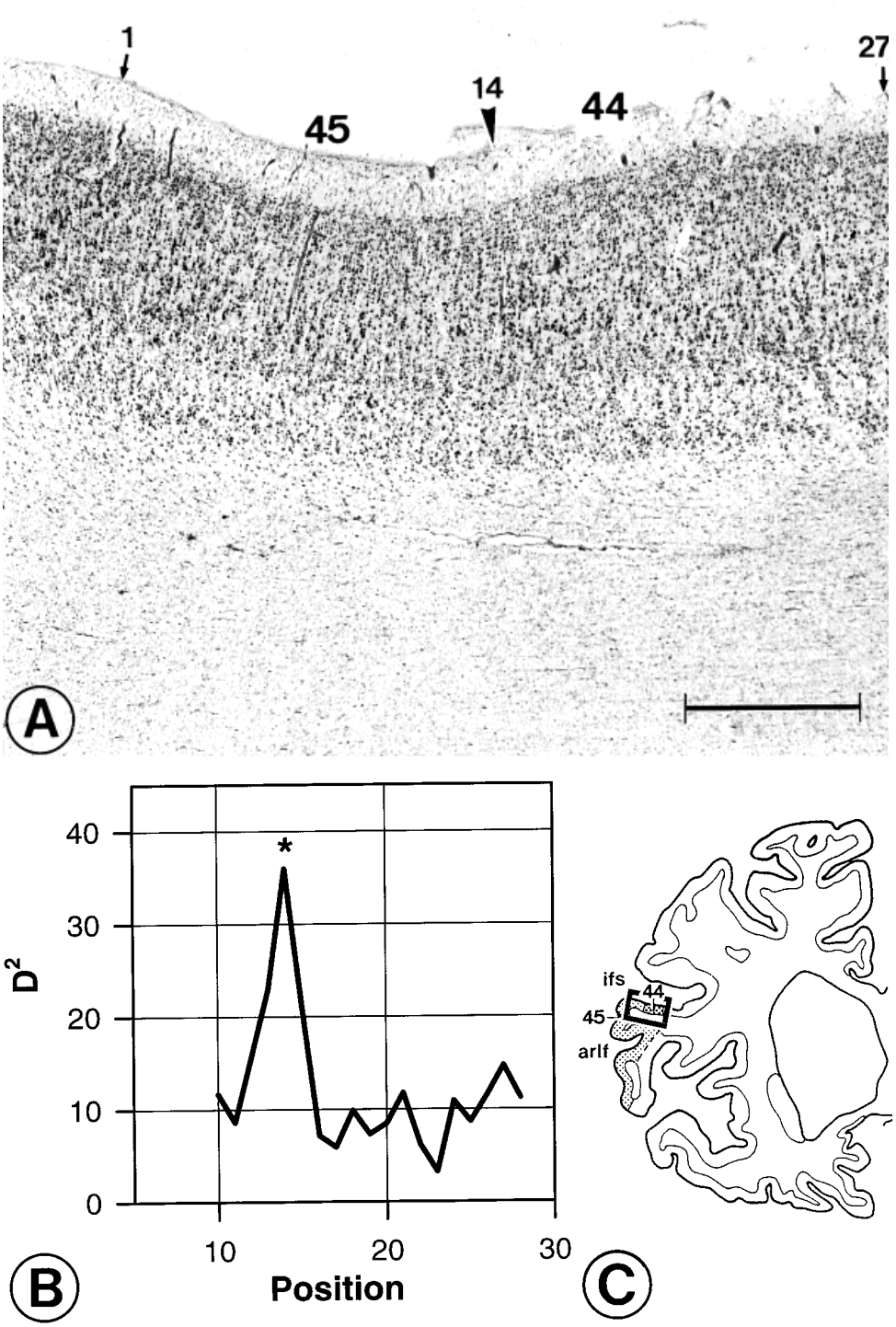

Fig. 5. Borders between areas 44 and 45 in a section of case 5 at position 14 (arrowhead) of the distance function. **A:** Photomicrograph of a coronal, cell body-stained section. Two positions of profiles at positions 1 and 27 are marked for orientation by small arrows. **B:** The significant peak of distance function D^2 at position 14 ($^*P < 0.05$) exactly matches the border. **C:** Location of the region of interest in the hemisphere. ifs, inferior frontal sulcus; arlf, ascending ramus of lateral fissure. Scale bar = 1 mm.

contrast, Economo and Koskinas (1925) found a series of cytoarchitectonic areas and their transitional forms in this region to be arranged in a caudorostral sequence. The mapping of the ventral–orbital surface outside Broca's region clearly needs further attention. Therefore, we have used only descriptive terms, e.g., "dysgranular area, ventral to area 44" (Fig. 11), for designating cytoarchitecture and approximate topography.

Figure 12 shows a rostrocaudal sequence of six histologic sections containing areas 44 and 45. It can clearly be seen

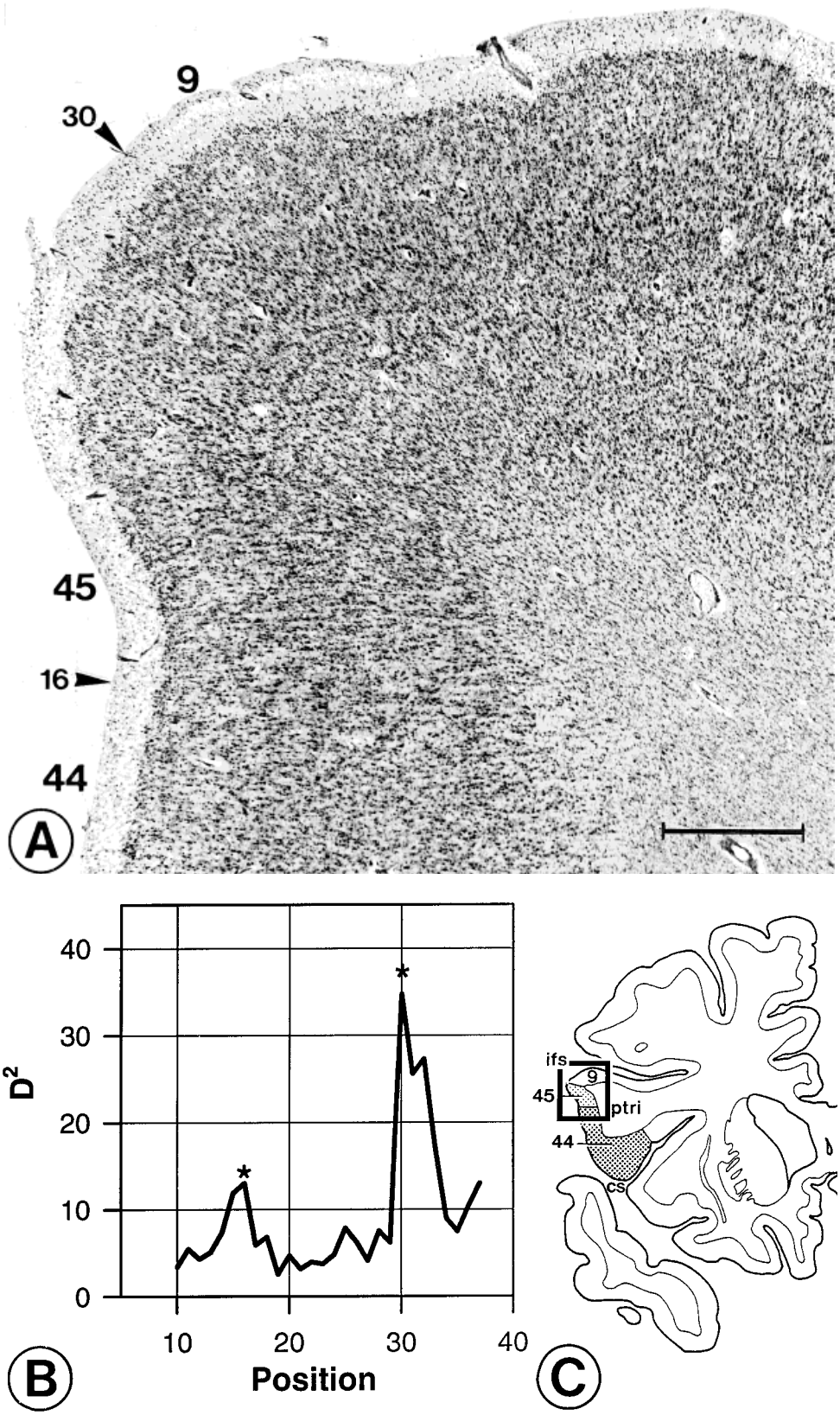

Fig. 6. **A:** Photomicrograph (case 9) showing borders between areas 44 and 45 and between areas 45 and 9 (marked by arrowheads). **B:** Two significant peaks (*$P < 0.05$) were found: at position 16 (between areas 44 and 45) and at position 30 (between areas 45 and 9). **C:** Location of areas and borders. ifs, inferior frontal sulcus; ptri, pars triangularis; cs, circular sulcus. Scale bar = 1 mm.

that the cytoarchitectonic borders did not coincide with reliably identifiable macroscopic features, e.g., with a fundus of a sulcus. Thus, macroscopic anatomy and areal borders differ independently.

Thickness of cortical layers and cell densities

Differences in relative thickness of cortical layers were not found between areas 44 and 45 with the exception of layer IV (ANOVA; significant interaction between the treatment factors area and layer; $F = 3.2$, $df = 3$, $P < 0.05$). Layer IV was relatively thicker in area 45 than in area 44 (Table 3). Gender- and side-dependent differences in relative layer thicknesses could not be detected ($P > 0.05$).

However, overall cell densities showed both gender-dependent and interhemispheric differences (two-way ANOVA). Cells bodies were more densely packed in the left than in the right area 44 (13.6%, S.E. = 0.57 vs. 12.7%, S.E. = 0.57; $F = 9.5$, $df = 1$, $P < 0.025$). The interaction between area and gender was not significant due to correction for multiple tests ($F = 5.6$, $df = 1$, $P > 0.025$). However, all five male brains showed a higher overall cell density in the left than in the right area 44. Thus, the AC of cell density was greater than zero in all male brains (Fig. 13). In contrast, three of five female brains showed a left-over-right asymmetry ($AC > 0$), but the remaining two showed a right-over-left asymmetry ($AC < 0$). The overall cell densities in area 45 did not show significant asymmetry or gender differences (Fig. 13).

Although significant differences were found between the cell density profiles of areas 44 and 45 in each subject (intrasubject, interareal differences), they could not be detected when mean profiles, collapsed over the entire sample (intersubject, interareal) were compared (Mahalanobis distance $D^2 = 10.03$, Hotelling $T^2 = 50.15$, $F = 2.5$, $df_1 = 10$, $df_2 = 9$, $P = 0.09$). A comparison of mean profiles averaged over the entire sample for areas 44 and of 45 is illustrated in Figure 14. This finding points to the large intersubject variability in the cytoarchitecture of each cortical area.

Intersubject variability in cytoarchitecture

We further analyzed intersubject variability in cytoarchitecture by calculating the Mahalanobis distance (D^2) between profiles of homologous areas in different brains (see section Interareal, interhemispheric, and gender coparisons of cytoarchitectonic parameters and volumes). The test showed large differences in the cytoarchitecture of area 44 across subjects (Fig. 15, left box). The same was found for area 45 (Fig. 15, middle box). Both D^2 values appeared to be significantly greater than those for the intrasubject differences between profiles of areas 44 and 45 in each single brain (Fig. 15, right box). Thus, intraareal (intersubject) differences in cytoarchitecture were greater than interareal differences in each individual brain ($P < 0.05$). These results were independent of side-of-hemisphere and gender.

Volumes of areas 44 and 45

We also found high intersubject variability in the volumes of both areas (Fig. 16). Volumes ranged from 920 mm^3 (area 44, right hemisphere, case 5) to 9,403 mm^3 (area 44, left hemisphere, case 3). Nevertheless (see S.D., below), there was a stable relationship between the volumes of area 44 on the left and right sides. Area 44 had, on average, a significantly greater volume on the left than on the right side (left: 3,839.9 mm^3, S.D. = 2,277.8 vs. right: 2,527.6 mm^3, S.D. = 1,597.9; $t = 5.4$, $df = 9$; $P < 0.001$). All 10 brains showed this leftward asymmetry. Side differences in area 45, however, were not significant (left: 3,242.1 mm^3, S.D. = 1,149.4 vs. right: 3,173.8 mm^3, S.D. = 1,637.7; $t = 0.1$, $df = 9$; $P > 0.025$). Gender differences in volume did not reach significance for either area 44 or 45. The absence of significant side differences in the volumes of area 45 was caused by differences in the direction of asymmetry across the 10 brains: five had larger volumes on the left and five had larger volumes on the right (Fig. 16).

Location of areas 44 and 45

We examined the position of Broca's region with respect to anatomic landmarks such as gyri and sulci. In all 10 cases, area 45 was present at the free cortical surface of the triangular part of the inferior frontal gyrus. It was located rostral to the ascending branch of the lateral fissure. Area 44 was always found on the free cortical surface of the opercular part of the inferior frontal gyrus. Lateral views of two 3-D reconstructed brains with the cytoarchitectonically defined areas are presented in Figure 17.

Areas 8, 9, 46, and 10 adjoin Broca's region rostrodorsally (Figs. 6 and 9 show examples of the border between areas 45 and 9; Fig. 10 shows an example of the border between areas 45 and 10; Fig. 7 shows an example of the border between areas 44 and 8). The dorsal border lies close to the inferior frontal sulcus in classic maps, but our analysis showed that its position in the sulcus differed across individuals. It may lie in the ventral or dorsal bank of the sulcus, but it never reached the free surface of the middle frontal gyrus. Intersubject differences in the position of the border in relation to the fundus of the inferior frontal sulcus reached 1.5–2 cm in sections cut perpendicular to the gyral surface. In addition, this sulcus was sometimes interrupted and thus consisted of several segments. In theses cases, it was not possible to correlate the position of the complete extent of the dorsal border with a consistent macroscopic feature such as the fundus of the sulcus.

The caudal border of area 44 adjoins area 6 (see also Fig. 8). The location of this border differed between the rostral and caudal walls of the precentral sulcus and thus differed with respect to the fundus by approximately 1–2 cm in this sample.

In most of the cases, the ventrorostral border of area 45 was located dorsal to the fundus of the horizontal branch of the lateral fissure and its continuation. In four hemispheres, however, this border was found on the ventral wall of the horizontal branch. In these cases, area 45 extended onto the orbital surface of the inferior frontal gyrus.

The border between areas 44 and 45 was located in the surrounding of the ascending branch of the lateral fissure in some hemispheres (Fig. 17B, right hemisphere). In others, it was close to the diagonal sulcus (Fig. 17A, right hemisphere) or even interposed between both sulci (Fig. 17A,B, left hemispheres). The diagonal sulcus was present in only nine of the 20 hemispheres. Even when the border between areas 44 and 45 was located in the diagonal sulcus, its exact position in relation to the fundus differed by approximately 1.5–2 cm.

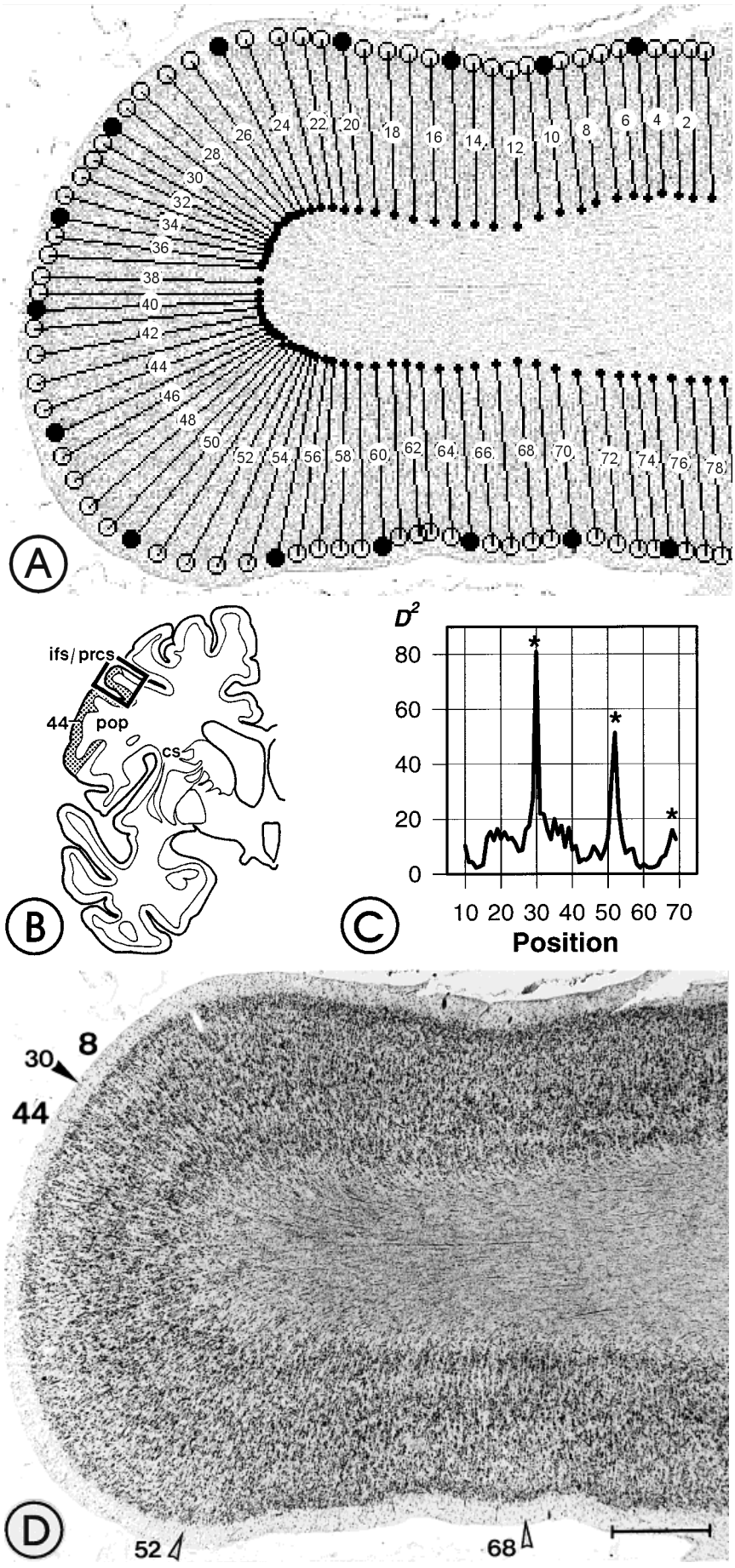

Figure 7

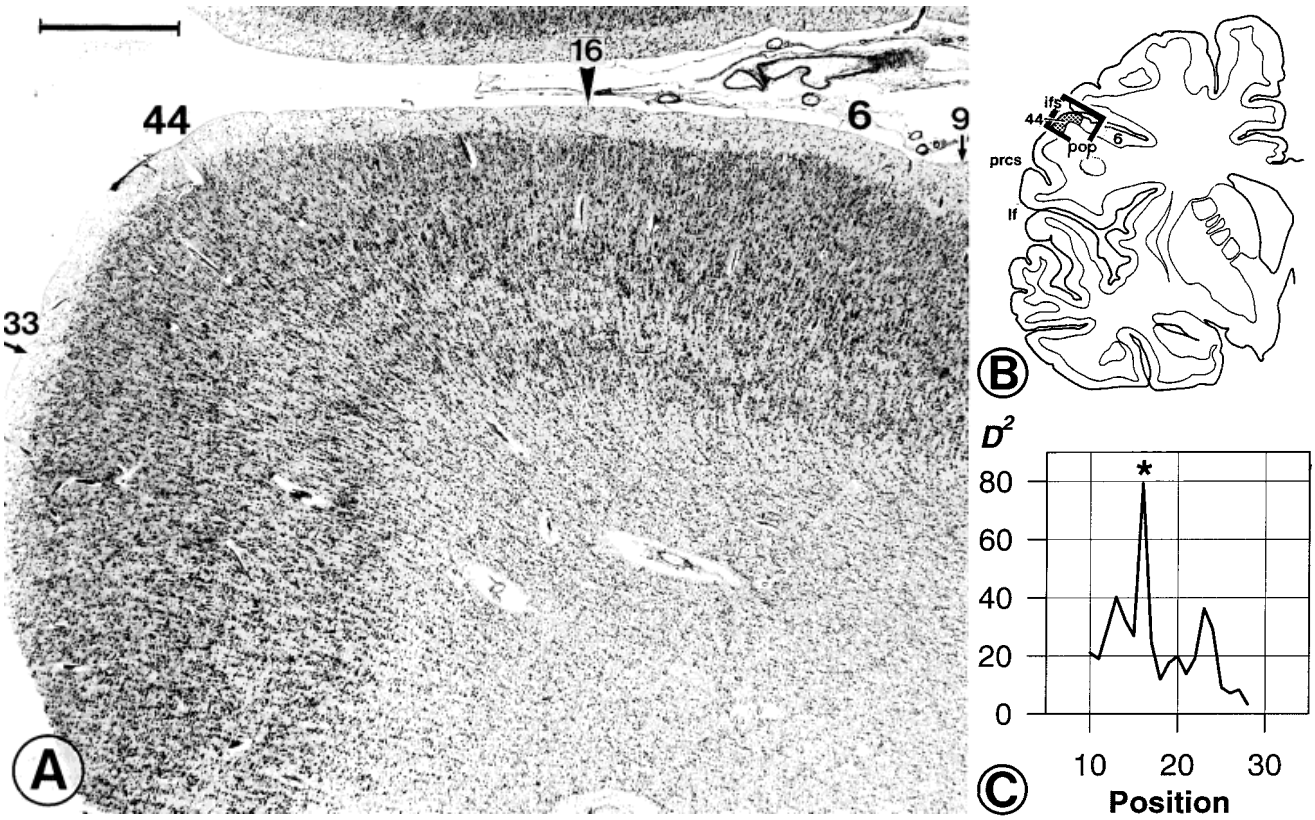

Fig. 8. Caudal border of area 44. **A:** Photomicrograph from case 1 showing the border between areas 44 and 6 (arrowhead). Small arrows indicate the positions of profiles 9 and 33 for orientation. **B:** Location of the region of interest. **C:** Significant maximum at position 16 (*$P <$ 0.05) indicates the border between areas 44 and 6. ifs, inferior frontal sulcus; lf, lateral fissure; pop, pars opercularis; prcs, precentral sulcus. Scale bar = 1 mm.

DISCUSSION

In the present study of Broca's region, a new observer-independent cytoarchitectonic technique was applied for determining areal borders. This technique has several advantages when compared with the traditional approach by pure visual inspection: the position and significance of borders can be statistically tested, and the technique is sensitive enough to detect subparcellations of cortical areas.

A few cytoarchitectonic borders, e.g., between the somatosensory cortex and the primary motor cortex and between the primary and secondary visual areas, are obvious and can be clearly defined by pure visual inspection. For these borders, discrepancies between different observers are marginal. However, the cytoarchitecture of the vast majority of cytoarchitectonic areas does not differ this distinctly ("homotypical isocortex" of Brodmann). Moreover, cytoarchitectonic features can change gradually at the transition between two areas. A well-known example is the gradual disappearance of giant pyramidal cells at the border between Brodmann's areas 4 and 6. Such cases led to the definition of "transitional areas" that share common cytoarchitectonic features with neighboring areas. One transitional area has been described at the border between prefrontal area 9 and area 45 (Rajkowska and Goldman-Rakic, 1995b). The observer-independent procedure localizes the precise position of the border even in such cases because the definition of borders is based on single and significant peaks in the multivariate distance function. This procedure allows one to identify a transitional area as a distinct cytoarchitectonic unit with reproducibly definable borders. A similar statistical approach is widely used in functional imaging studies because clusters of activation are considered meaningful only if there are significant differences between signal and "noise" (Roland, 1993; Cherry and Phelps, 1996; Friston, 1996). Moreover, the analysis of cell density profiles in a transition area makes it possible to objectively define the degree of similarity between the cytoarchitecture of the transition area and the surrounding areas. The transition area may then be clearly classified according to the similarity criterion as a subarea of one of the neighboring areas.

Fig. 7. Subdivision of area 44 in case 4. **A:** Gray level image from the pars opercularis, with the positions of the profiles numbered consecutively from 1 to 79. **B:** Location of the region of interest. **C:** The distance function D^2 showed significant borders between areas 44 and 8 at position 30 and within area 44 at positions 52 and 68 (*$P < 0.05$). Note that the small rupture of the tissue, which is located between positions 25 and 26, does not cause an artificial border. **D:** Corresponding photomicrograph with borders between areas 44 and 8 (filled arrowhead) and within area 44 (open arrowheads). cs, circular sulcus; ifs/prcs, transition between inferior frontal and precentral sulcus; pop, pars opercularis. Scale bar = 1 mm.

Methodologic considerations

The multivariate distance function between groups of profiles was calculated to quantify the degree of differences

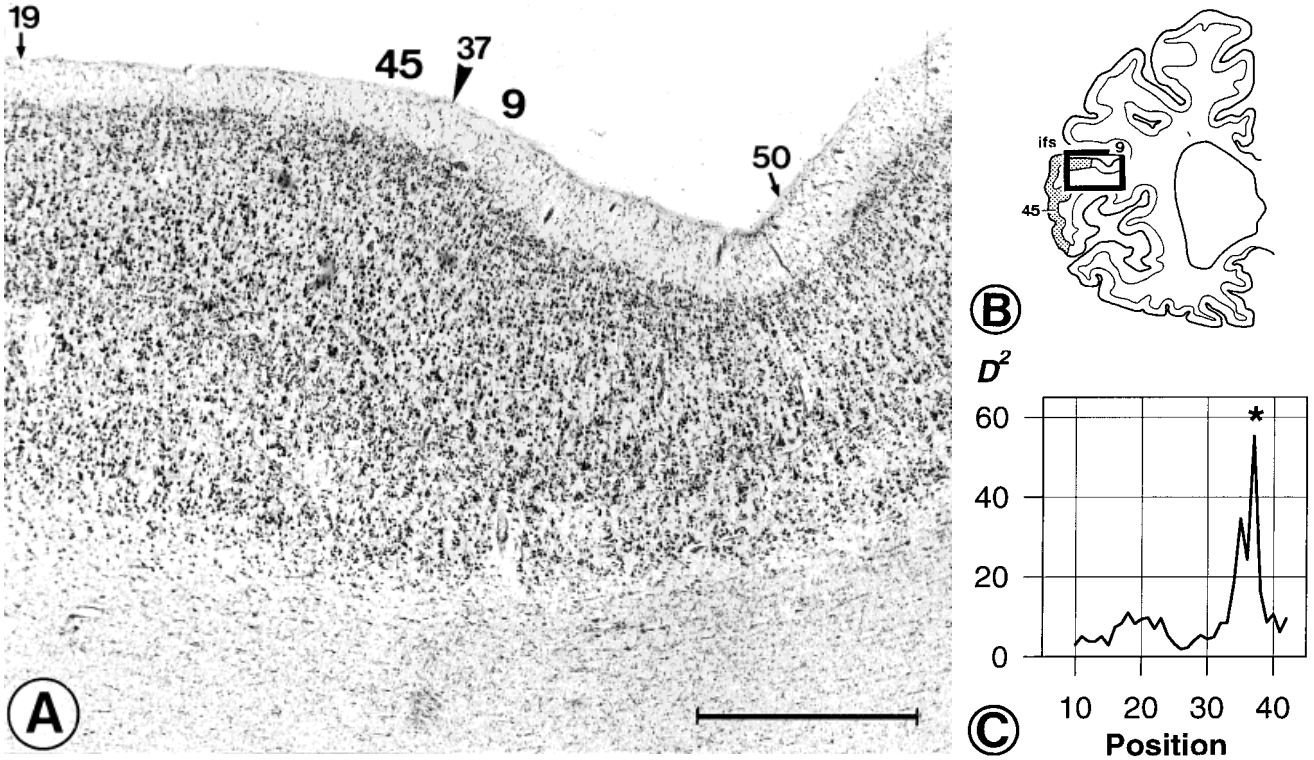

Fig. 9. Dorsal border of area 45. **A:** Photomicrograph from case 5 showing the border between areas 45 and 9 (arrowhead). Small arrows indicate positions of profiles 19 and 50 for orientation. **B:** Location of the region of interest. **C:** Significant maximum at position 37 (*$P <$ 0.05) indicates border between areas 45 and 9. ifs, inferior frontal sulcus. Scale bar = 1 mm.

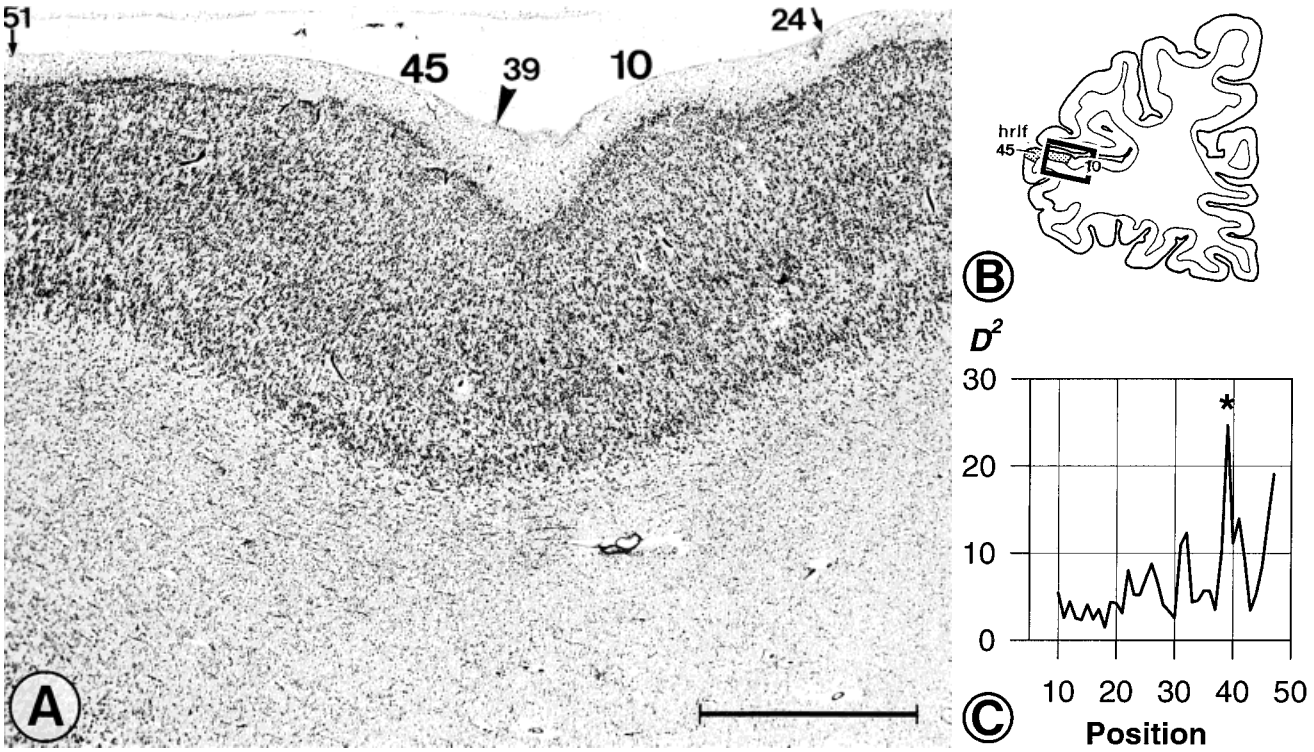

Fig. 10. Rostral border of area 45. **A:** Photomicrograph of a section from case 3 showing the border between areas 45 and 10 (arrowhead). Small arrows indicate positions of profiles 24 and 51. **B:** Location of the region of interest. **C:** Significant maximum at position 39 (*$P < 0.05$) indicates the border between areas 45 and 10. hrlf, horizontal ramus of the lateral fissure. Scale bar = 1 mm.

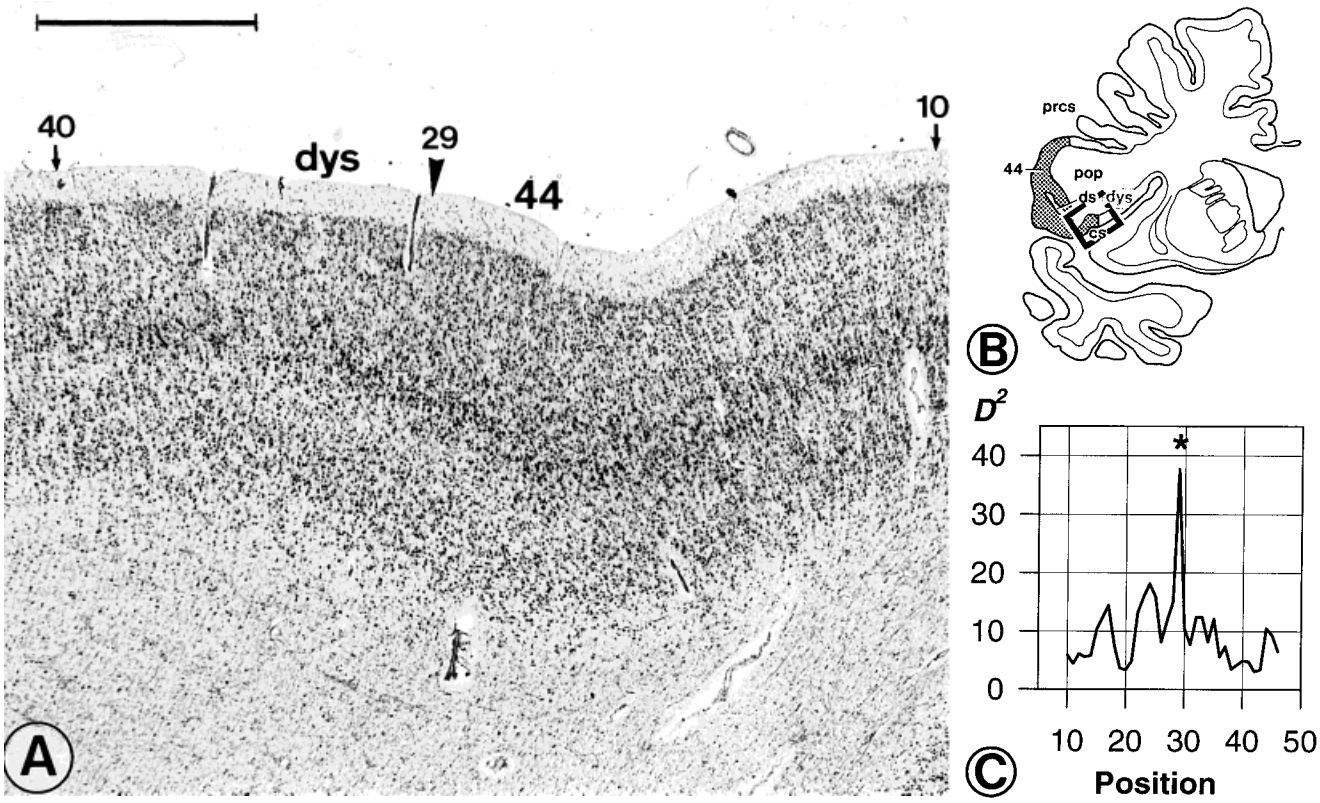

Fig. 11. Ventral border of area 44. **A:** Photomicrograph of a section from case 8 showing the ventral border of area 44 (arrowhead). Small arrows indicate positions of profiles 10 and 40. **B:** Location of areas and borders. **C:** Significant maximum at position 29 ($*P < 0.05$) indicates the border between areas 44 and the dysgranular cortex located ventral to area 44. cs, circular sulcus; ds, diagonal sulcus; dys, dysgranular cortex located ventral to area 44; pop, pars opercularis; prcs, precentral sulcus. Scale bar = 1 mm.

in laminar distribution patterns between areas. Previous studies have shown that the Mahalanobis distance is superior to other distance measures, e.g., the Euclidean distance (Schleicher et al., 1995, 1998). It is possible to apply the method to all structures with a lamination pattern and, therefore, is not limited to the human cerebral cortex. The method can also be applied for identifying borders in chemo- and myeloarchitectonic specimens (Jansen et al., 1996). The analysis of the distance function shows local but not long-term shifts in architecture (Schleicher et al., 1998). The sharp and not gradually changing character of myeloarchitectonic borders of the inferior frontal gyrus had been established (Vogt and Vogt, 1919) and was subsequently confirmed for cytoarchitecture (Riegele, 1931).

The application of the automated delineation procedure in most cases showed borders of areas 44 and 45 at positions that were in good agreement with results obtained by pure visual inspection. In other cases, borders could not be reliably and convincingly defined by visual inspection. The present approach provided reproducible and statistically significant borders even in these cases. The application of the automated delineation procedure requires very homogeneous staining of high contrast, which is achieved with the silver-staining technique used in our laboratory. Small artifacts, as illustrated in some of the figures, did not result in "artificial" borders. However, even if large artifacts cause "artificial" peaks on the distance function, statistically significant peaks are interpreted as cytoarchitectonic borders only if they occur in adjacent sections. A staining artifact, a rupture of the tissue, or a large blood vessel may distort the distance function in one section but do not appear over many sections.

To apply the automated procedure, it is necessary that the histologic sections contain the entire ROI. Ideally, the plane of sectioning should not be too oblique. In the case of gyrificated brains, it is inevitable that some parts of the ROI are obliquely sectioned. Although this condition must also be fulfilled in classic cytoarchitectonic studies, it is an important methodologic result that our automated delineation was relatively resistant to variations in sectioning planes. It was found that cortical thickness in oblique planes should not be more than two to three times larger than if the same area had been sectioned exactly parallel to the cell columns. It is clear that no delineation can be achieved either by visual inspection or with the automated method when not all cortical layers are present in a section, e.g., when the fundus of a sulcus or the crown of a gyrus is cut tangentially.

Cytoarchitecture and intersubject variability of areas 44 and 45

Although the laminar distribution patterns differed significantly between areas 44 and 45 in each brain, no

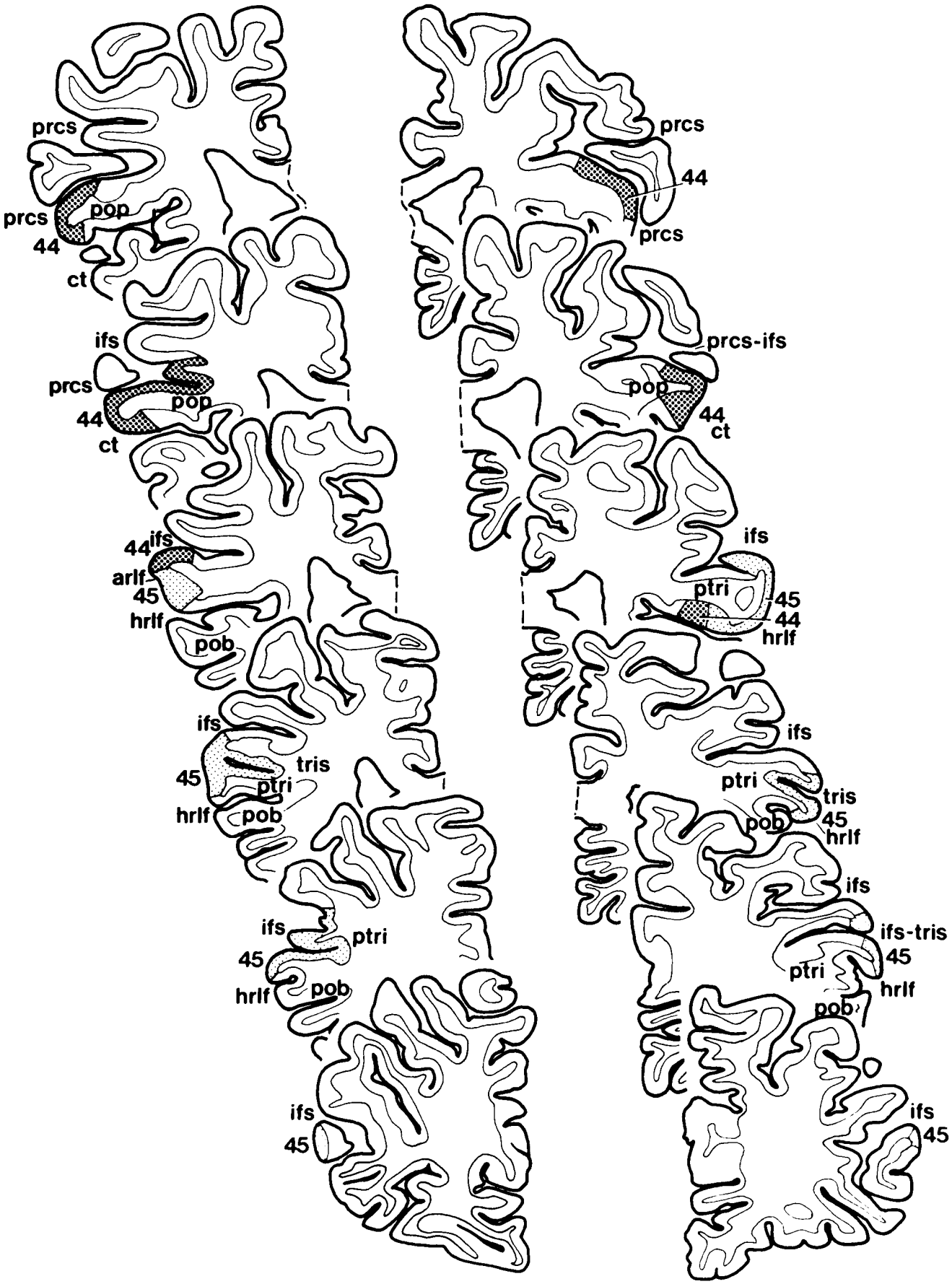

Figure 12

TABLE 3. Relative Thickness[1] of Cortical Layers ± S.D. (%)

Layer	Area 44	Area 45
II	9.5 ± 1.1	9.5 ± 1.2
III	33.9 ± 4.6	34.0 ± 2.9
IV	8.7 ± 1.1	10.9 ± 1.3
V	19.9 ± 2.3	18.9 ± 2.1
VI	28.0 ± 4.4	26.7 ± 3.0

[1]The relative thickness of each layer is calculated after normalizing the distance between the layer I/II border and the cortex/white matter border. Because left–right differences were not significant ($P > 0.05$), means of the measurements in both hemispheres are presented.

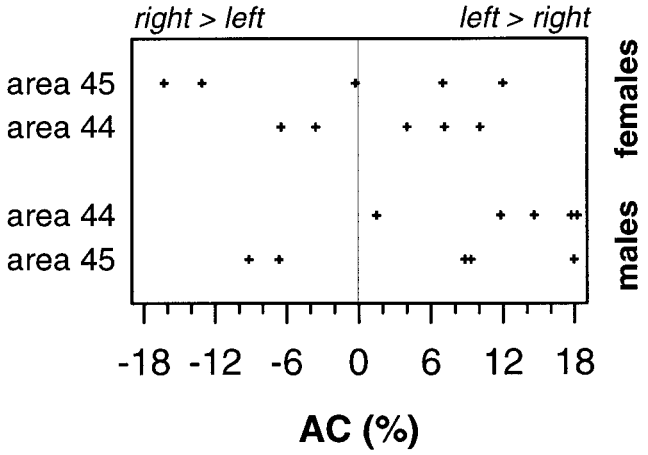

Fig. 13. Asymmetry coefficient (AC, %) of overall density of cell bodies (gray level index) collapsed over all cortical layers in areas 44 and 45 of male (lower half) and female (upper half) brains. All five male brains showed a left-larger-than-right asymmetry in area 44. By contrast, the ACs for females in area 44 and for both sexes in area 45 were more evenly distributed, i.e., no interhemispheric asymmetry could be detected in these cases.

such differences were found when the profiles of both areas were compared for the whole sample because high intersubject variability smoothed the cytoarchitectonic differences between the areas. In addition, the cytoarchitecture of both areas is rather similar. Common cytoarchitectonic features of areas 44 and 45 include prominent pyramidal cells in deep layer III and in layer V, the lack of a clear border between layers II and III, and the low cell density in layer VI. Areas 44 and 45 can be distinguished mainly because layer IV in area 45 is relatively more distinct than that of "dysgranular" area 44 (Riegele, 1931). Our analysis of relative layer thickness in both areas supports this statement. Layer IV was relatively thinner in area 44 despite our definition of layer IV, which included some invading pyramidal cells from layers III and V. This difference was statistically significant.

Fig. 12. Drawings of coronal sections of frontal cortex through the left and right hemispheres of case 10. The left hemisphere is on the left, the right on the right. Sections were taken from six different rostrocaudal levels (sections 5191, 5341, 5536, 5715, 5881, 6076). Areas 44 and 45 are shown by dark and light hatch marks, respectively. arlf, ascending ramus of the lateral fissure; cs, circular sulcus; ct, common trunk of arlf and hrlf; ds, diagonal sulcus; ifs, inferior frontal sulcus; hrlf, horizontal ramus of the lateral fissure; pob, pars orbitalis; pop, pars opercularis; prcs, precentral sulcus; prcs-ifs, transition between ifs and prcs; ptri, pars triangularis; tris, triangular sulcus.

Intersubject variability in human brain anatomy is influenced by factors such as heredity, gender, age, brain size and shape, life history, clinical history, cause of death, and autopsy conditions (Vierordt, 1893; Blinkov and Glezer, 1968; Haug, 1980; Skullerud, 1985). Variability in structure may contribute to variability in speech production and to the intensity of a deficit or recovery after stroke (Mohr, 1973). Economo and Koskinas (1925) noted pronounced intersubject variability in the microstructure, e.g., in the size of the large pyramidal cells in deep layer III and their presence in area FCBm. The clarity of the borders of Broca's region to areas of the middle frontal gyrus also differed (Economo and Koskinas, 1925). Intersubject differences in the sizes of areas 44 and 45 were also described (Kononova, 1935; 1949). In the present analysis, we compared the differences in cytoarchitecture between the homologous areas in different individuals (intersubject variability) with the differences between them in each single case (interareal variability). Intersubject differences between areas 44 and between areas 45 were larger than intrasubject differences between areas 44 and 45 in each individual brain. One may argue that shrinkage affected the brains to different degrees during histologic procedures and may have influenced absolute cell density and thus the profiles. However, the GLI is not a measure of absolute cell density; it is a ratio describing the volume proportion occupied by cell bodies in a certain volume of cortical tissue. Therefore, the GLI is not influenced by shrinkage if both major compartments (cell bodies and neuropil) shrink to the same or nearly the same degree. Maximal differences in shrinkage between the gray matter (containing relatively more cell bodies than fibers) and the white matter (containing relatively fewer cell bodies and more fibers) of only 9% has been reported (Kretschmann et al., 1982). Thus, differential shrinkage cannot explain high intersubject variability.

Intersubject variability in cytoarchitecture was accompanied by intersubject variability in the positions of areas 44 and 45 relative to sulci and gyri. We found that one and the same cytoarchitectonic border was located in a sulcal fundus in some hemispheres but on one or the other wall of the sulcus or at the top of a gyrus in others. Distances from the fundus of up to 1.5–2 cm were observed. The spatial variability of borders relative to macroscopic features therefore is a relevant factor for the architectonic interpretation of functional imaging studies with a spatial resolution of a few millimeters. The classic maps do not provide information concerning the position of borders in the depths of a sulcus. Kononova (1938) found areal borders of areas 44 and 45 that did not coincide with the fundus of a sulcus. In some sections, area 45 does not reach the inferior frontal sulcus; in other sections, area 45 occupies parts of the dorsal wall of the middle frontal gyrus (Kononova, 1938).

In addition, there is great variability among the smaller but important sulci of the inferior frontal gyrus (Ono et al., 1990; Duvernoy, 1991; Kretschmann and Weinrich, 1996). For example, the diagonal sulcus and the triangular sulci may or may not be present, and the courses of the horizontal and ascending branches of the lateral fissure may differ. There are pronounced individual differences in the continuity or discontinuity of the inferior frontal sulcus and the courses of the precentral sulcus (Ono et al., 1990; Duvernoy, 1991). Furthermore, we found that the diagonal sulcus can either be located within area 44 or

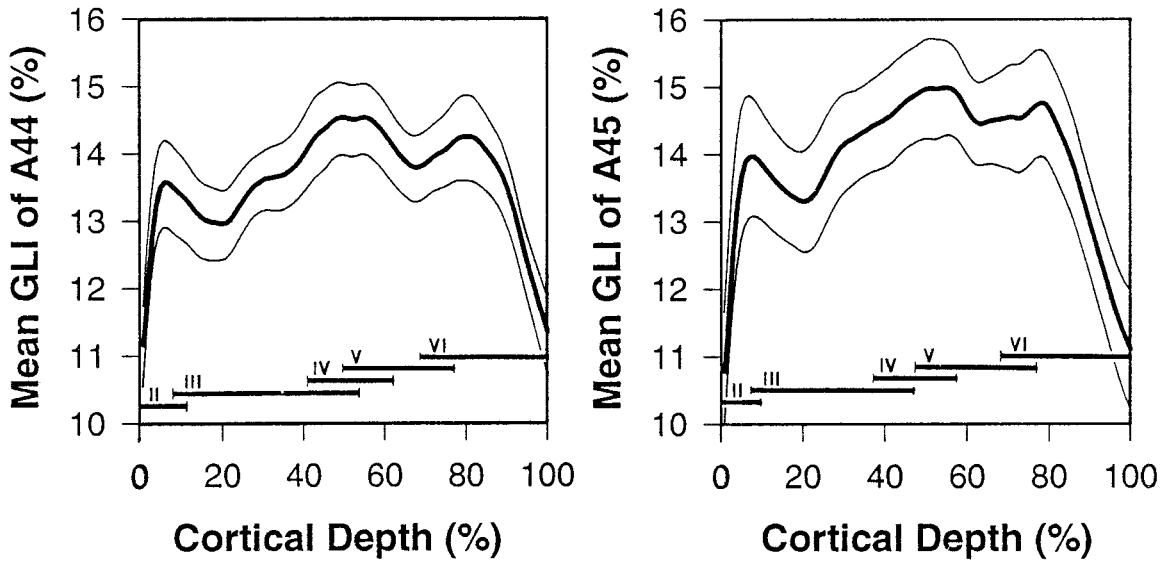

Fig. 14. Mean profiles of all subjects (gray level index, GLI; mean ± S.E.; n = 10, left hemispheres) in areas 44 and 45 showing laminar changes in cell density from the border between layers I and II (abscissa, 0%) to the white matter (abscissa, 100%). The ranges where the borders of cortical layers are found are marked by thin horizontal lines above the abscissa. Roman numerals, numbers of layers. In contrast to the situation shown in Figure 3, the shapes of profiles obtained from areas 44 and 45 seem to be similar when averaged over the entire sample.

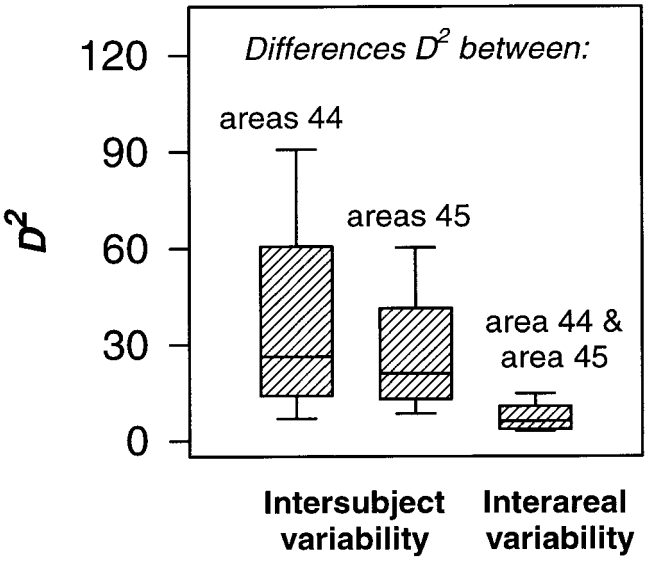

Fig. 15. Intersubject and interareal variabilities in shape of the gray level index profiles. Box plots show median (center horizontal), first and third quartiles (upper and lower edges of the box), and 10 and 90 percentiles (vertical lines above and below the box) of Mahalanobis distances (D^2) in area 44 (left, n = 45), area 45 (middle, n = 45), and area 44 versus area 45 (right, n = 10). The first two boxes indicate interindividual differences, the last one shows interareal differences in cytoarchitecture within the same brain. Differences between mean interareal D^2 and mean interindividual D^2 were significant ($P < 0.05$).

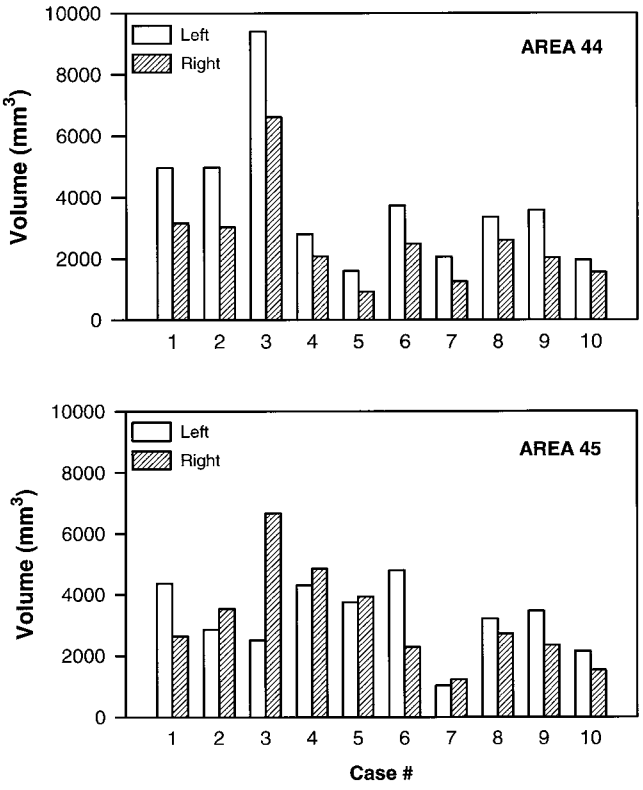

Fig. 16. Volumes (mm^3) of left and right areas 44 and 45. Side differences for area 44 were highly significant ($P < 0.001$). Side differences for area 45 were not significant ($P > 0.05$).

mark the border between areas 44 and 45 (for further comparison, see Economo and Koskinas, 1925; Kononova, 1949; Braak, 1979; Galaburda, 1980). A similar lack of correspondence between a sulcus and a cytoarchitectonic area has been reported for the horizontal branch of the lateral fissure and its relationship to area 45 (Kononova, 1935, 1949). Riegele (1931) found that cytoarchitectonic areas of the opercular part of the inferior frontal gyrus may be shifted with respect to a certain sulcus by one

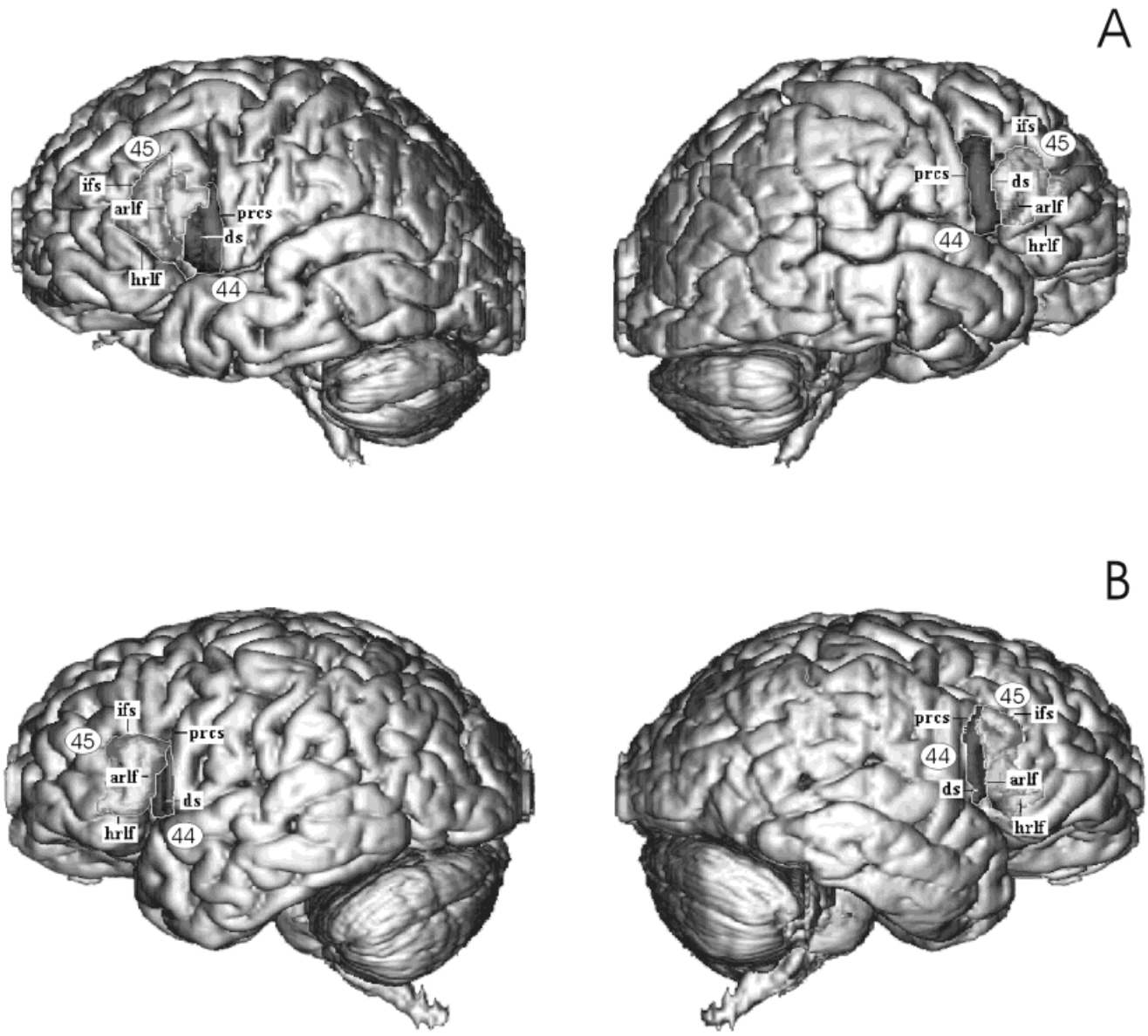

Fig. 17. Lateral views of two three-dimensional reconstructed brains of cases 8 and 9. Volumes of areas 44 and 45 (dark and light hatch marks, respectively) were projected onto lateral surfaces. **A:** Left and right hemispheres of case 8. **B:** Left and right hemispheres of case 9. arlf, ascending ramus of lateral fissure; ds, diagonal sulcus; ifs, inferior frontal sulcus; hrlf, horizontal ramus of lateral fissure; prcs, precentral sulcus.

gyrus. He concluded that it is not possible to define the location of a cytoarchitectonic area precisely based on macroscopic landmarks.

This variability of cytoarchitectonic areas can be interpreted as class 1 variability that is not predictable from visible landmarks (Rademacher et al., 1993). In contradistinction, class 2 variability is predictable from visible landmarks. A prevalence of class 2 variability was found in four primary cortical areas, i.e., these areas were found to bear a characteristic relationship to a set of landmarks. Therefore, the landmarks that frame these fields may be a more reliable basis for functional imaging than referring to a stereotactic system (Rademacher et al., 1993). However, areas 44 and 45 do not belong to primary areas. They did not show this close relationship to sulci in the present sample. Thus, landmark-based anatomic interpretations of functional data of Broca's region are possible only in those particular cases in which foci of activation match the free surfaces of the opercular and/or triangular parts. Interpretations become more and more inaccurate the smaller the distance to a "bordering" sulcus.

The present study has demonstrated the presence of parcellations within areas 44 and 45. Thus, neither area seems to be completely homogeneous cytoarchitectonically. Subdivisions of areas 44 and 45 have been described in the past but have not been systematically examined. Economo and Koskinas (1925) recognized a "campus anterior" and "campus posterior" in area 44, which were separated by

the diagonal sulcus. The anterior part had a thinner cortex, fewer pyramidal cells in layer IIIc, and a paler layer Vb than did the posterior part. This anterior–posterior divergence in cytoarchitecture, with the diagonal sulcus as an internal border, was corroborated in subsequent independent studies (Kononova, 1935, 1949). However, this subdivision of area 44 requires the presence of the diagonal sulcus, which is not found in all brains. Several cytoarchitectonic subdivisions have been found within area 45 (Kononova, 1949). Myeloarchitectonic (Petrides and Pandya, 1994) and pigment-architectonic observations (Braak, 1979) also have described possible subdivisions within areas 44 and 45 (Vogt, 1910). Similar subdivision of areas 44 and 45 have been found in *Macaca mulatta* (Petrides and Pandya, 1994). However, it is still under discussion as to which cortical areas are the homologues of human areas 44 and 45 in the monkey (Lieberman, 1985; Barbas and Pandya, 1987; Aboitiz and Garcia, 1997; Rizzolatti and Arbib, 1998). Of the areas composing Broca's region, only area 45 has been confirmed by Preuss and Goldman-Rakic (1991).

Functional imaging studies in man also have provided some evidence concerning a subparcellation of both areas. Positron emission tomography during different tasks of phonetic processing have shown cortical activations that were probably located in a posterior and superior subregion of area 44 near the border with area 6 but not in the inferior part of area 44 (Zatorre et al., 1996). Another study found a cluster of cortical activation in the most posterior and ventral subregion of area 44 (Amunts et al., 1998). In conclusion, architectonic and functional data strongly suggest that areas 44 and 45 are heterogeneous. The systematic anatomic mapping of these subareas and an analysis of their functional significance require further detailed studies.

Anatomic left–right and gender differences in Broca's region

In contrast to a large number of reports on structural asymmetries in the posterior speech region, i.e., in Wernicke's area (Flechsig, 1920; Pfeifer, 1920; Economo and Horn, 1930; Geschwind and Levitsky, 1968; Witelson and Pallie, 1973; Sanides, 1975; Chi et al., 1977; Galaburda and Geschwind, 1981; Galaburda et al., 1987; Steinmetz et al., 1991; Witelson and Kigar, 1992; Jacobs et al., 1993b; Jacobs and Scheibel, 1993; Schlaug et al., 1995a; Anderson and Rutledge, 1996; Ide et al., 1996; Penhune et al., 1996; Steinmetz, 1996), such asymmetries in the anterior speech region have only rarely been examined. For review, see Uylings et al. (1999).

The present study has shown interhemispheric differences in the GLI for area 44. The GLI was higher on the left than on the right. This finding indicates that there was more space between cell bodies (i.e., the neuropil) in the right than in the left area 44. Corresponding left–right differences have been described for dendrites that form a major part of the neuropil; a greater total dendritic length per neuron was found in the right than in the left Broca area (Jacobs et al., 1993a). The right opercular region showed longer lower-order dendritic segments than did the left opercular region (Scheibel, 1984). In contrast to area 44, we did not find any significant left–right differences in GLI in area 45. This lack of asymmetry is compatible with other reports. For example, the sizes of magnopyramidal cell bodies in area 45 were similar for both hemispheres, and only the largest magnopyramidal cells of layer III were found to be larger on the left than on the right (Hayes and Lewis, 1995, 1996).

The present study has also shown that differences in GLI between the left and right areas 44 seem to be gender dependent. Whereas the GLI, which is a good estimate of cell packing density (Wree et al., 1982), was consistently higher on the left in all male brains, only three of five female brains showed this asymmetry. Other anatomic gender differences in Broca's region have been reported. The volume of a region roughly corresponding to the opercular, triangular, and orbital parts were found to differ between male and female brains, but side differences were not detectable (Harasty et al., 1997). An MR imaging study has shown a higher percentage of gray matter ventral to the dorsolateral prefrontal cortex in women than in men, but it did not examine left–right differences (Schlaepfer et al., 1995). Male brains tended to have a more distinctly asymmetric sulcal pattern in the posterior part of the Sylvian fissure but not in the anterior part including Broca's region (Witelson and Kigar, 1992). Gender differences in the functional lateralization of language have been found in both lesion and functional imaging studies (McGlone, 1980; Kimura, 1983; Hier et al., 1994; Pedersen et al., 1995; Shaywitz et al., 1995). The study by Shaywitz et al. (1995) has shown that brain activation of the inferior frontal gyrus during particular phonological tasks is more lateralized in male than in female brains. However, it is still an open question as to whether these side differences can be assigned to area 44, area 45, or both.

The interhemispheric differences in the volume of area 44 appear to be greater than those in cytoarchitecture. A left-over-right asymmetry was detected in all 10 cases. This finding supports an that of a previous study in which a significantly larger area 44 was found on the left than on the right (Galaburda, 1980). Nine of the 10 subjects of that study had a larger area 44 on the left side. If the present sample is combined with that in the study by Galaburda, the incidence of leftward asymmetry (19 of 20 cases, 95%) matches the frequency of left-sided speech dominance in the general population (Branche et al., 1964) and may structurally reflect the functional lateralization (Steinmetz et al., 1991; Annett and Alexander, 1996). In the present study, no consistent left–right difference in the volume of area 45 was found. Five cases showed left-over-right asymmetry and the other right-over-left asymmetry. The degree of asymmetry (without considering sides) did not differ significantly between the two areas. Thus, area 45 is not more symmetric than area 44; it is more heterogeneous pertaining to the direction of asymmetry. The data on volumes of areas 44 and 45 also clearly showed that the variability of this parameter and of the total brain weights (and, thus, brain volumes) are considerable. Because a preliminary ontogenetic study in six female and five male brains indicated a left-over-right asymmetry in the volume of area 45 in the male group (Uylings et al., 1999), further studies on a larger number of male and female subjects is needed to show the pattern of asymmetry in area 45.

In previous studies on asymmetry, the sulcal patterns were used to mark the border of the speech region (Stengel, 1930). A left-over-right asymmetry was found when both extra- and intrasulcal parts of the cortex were combined (Falzi et al., 1982). A similar asymmetry was found in the pars triangularis (Albanese et al., 1989; Foundas et al., 1995).

In conclusion, the asymmetry we found in the cytoarchitecture and volume of area 44 could well be the structural correlate of speech lateralization. Area 45 seems to be less lateralized. Area 44, but not 45, was also asymmetric with respect to cell packing density, and this feature differed between genders. We have shown that, because both the sulcal pattern and the cytoarchitectonic borders of Broca's region are highly and independently variable, areas 44 and 45 cannot be reliably and precisely localized on the basis of contours seen in MR images. There are regions, i.e., the free surfaces of the triangular and opercular parts, in which the probability is very high of localizing areas 45 and 44, respectively. However, the smaller the distance to surrounding sulci, the greater the probability of finding areas other than these. Thus, anatomic interpretation becomes much more accurate when images containing functionally characterized areas are warped into atlases containing 3-D representations of cytoarchitectonically mapped areas because these atlases may quantify the probability of localizing a specific area at a given stereotaxic position (Roland and Zilles, 1994, 1996, 1998; Zilles et al., 1995). Three-dimensional probability maps of areas 44 and 45 can be applied for analyzing the role of Broca's region in speech and in functions that are different from speech (Amunts et al., 1998).

ACKNOWLEDGMENTS

We thank Per E. Roland for helpful discussions and Kristina Rascher for editorial assistance. We are grateful to Christine Opfermann-Rüngeler for the art work and Ursula Blohm and Brigitte Machus for expert technical assistance.

LITERATURE CITED

Aboitiz F, Garcia GL. 1997. The evolutionary origin of language areas in the human brain. A neuroanatomical perspective. Brain Res Rev 25:381–396.

Albanese E, Merlo A, Albanese A, Gomez E. 1989. Anterior speech region. Asymmetry and weight–surface correlation. Arch Neurol 46:307–310.

Amunts K, Schlaug G, Schleicher A, Steinmetz H, Dabringhaus A, Roland PE, Zilles K. 1996. Asymmetry in the human motor cortex and handedness. Neuroimage 4:216–222.

Amunts K, Schlaug G, Jäncke L, Steinmetz H, Schleicher A, Zilles K. 1997. Motor cortex and hand motor skills: structural compliance in the human brain. Human Brain Mapping 5:206–215.

Amunts K, Klingberg T, Binkofski F, Schormann T, Seitz RJ, Roland PE, Zilles K. 1998. Cytoarchitectonic definition of Broca's region and its role in functions different from speech. Neuroimage 7:8.

Anderson B, Rutledge V. 1996. Age and hemisphere effects on dendritic structure. Brain 119:1983–1990.

Annett M, Alexander MP. 1996. Atypical cerebral dominance: predictions and tests of the right shift theory. Neuropsychologia 34:1215–1227.

Barbas H, Pandya DN. 1987. Architecture and frontal cortical connections of the premotor cortex (area 6) in the rhesus monkey. J Comp Neurol 256:211–228.

Berrebi AS, Fitch RH, Ralphe DL, Denenberg JO, Friedrich J, Denenberg VH. 1988. Corpus callosum: region-specific effects of sex, early experience and age. Brain Res 438:216–224.

Binder JR, Swanson SJ, Hammeke TA, Morris GL, Mueller WM, Fischer M, Benbadis S, Frost JA, Rao SM, Haughton VM. 1996. Determination of language dominance using functional MRI: a comparison with the Wada test. Neurology 46:978–984.

Blinkov SM, Glezer II. 1968. Das Zentralnervensystem in Zahlen und Tabellen. Jena: Fischer.

Bonin Gv, Bailey P. 1961. Pattern of the cerebral isocortex. Primatologia. Basel: Karger.

Botez MI, Wertheim N. 1959. Expressive aphasia and amusia following right frontal lesion in a right-handed man. Brain 82:186–202.

Braak H. 1979. The pigment architecture of the human frontal lobe. Anat Embryol 157:35–68.

Bradvik B, Dravins C, Holtas C, Rosen I, Ryding E, Ingvar DH. 1991. Disturbances of speech prosody following right hemisphere infarcts. Acta Neurol Scand 84:114–126.

Branche C, Milner B, Rasmussen T. 1964. Intracarotid sodium amytal for the lateralization of cerebral speech dominance. J Neurosurg 21:399–405.

Braun AR, Varga M, Stager S, Schulz G, Selbie S, Maisog JM, Carson RE, Ludlow CL. 1997. Altered patterns of cerebral activity during speech and language production in developmental stuttering. An H2 15O positron tomography study. Brain 120:761–784.

Broca MP. 1861. Remarques sur le siége de la faculté du langage articulé, suivies d'une observation d'aphemie (Perte de la Parole). Bull Mem Soc Anat Paris 36:330–357.

Brodmann K. 1909. Vergleichende Lokalisationslehre der Großhirnrinde in ihren Prinzipien dargestellt auf Grund des Zellenbaues. Leipzig: Barth JA.

Brown J. 1972. Aphasia, apraxia and agnosia. Springfield: Charles C. Thomas.

Buckner RL, Corbetta M, Schatz J, Raichle ME, Petersen SE. 1996. Preserved speech abilities and compensation following prefrontal damage. Proc Natl Acad Sci USA 93:1249–1253.

Caplan D, Hidebrandt N, Makris N. 1996. Location of lesions in stroke patients with deficits in syntactic processing in sentence comprehension. Brain 119:933–949.

Cherry SR, Phelps ME. 1996. Imaging brain function with positron emission tomography. In: Toga AW, Mazziotta JC, editors. Brain mapping. The methods. San Diego: Academic Press. p 191–221.

Chi JG, Dooling EC, Gilles FH. 1977. Left–right asymmetries of the temporal speech areas of the human fetus. Arch Neurol 34:346–348.

Damasio AR. 1992. Aphasia. N Engl J Med 326:531–539.

Demonet JF, Chollet F, Ramsay S, Cardebat D, Nespoulous JL, Wise R, Rascol A, Frackowiak RSJ. 1992. The anatomy of phonological and semantic processing in normal subjects. Brain 115:1753–1768.

Desmond JE, Sum JM, Wagner AD, Demb JB, Shear PK, Glover GH, Gabrieli JE, Morrell MJ. 1995. Functional MRI measurement of language lateralization in Wada-tested patients. Brain 118:1411–1419.

Duvernoy H. 1991. The human brain. Surface, three-dimensional sectional anatomy and MRI. New York: Springer.

Economo Cv, Horn L. 1930. über Windungsrelief, Maße und Rindenarchitektonik der Supratemporalfläche, ihre individuellen und ihre Seitenunterschiede. Zeitschr Neurol Psychiatrie 130:678–757.

Economo Cv, Koskinas GN. 1925. Die Cytoarchitektonik der Hirnrinde des erwachsenen Menschen. Berlin: Springer.

Falzi G, Perrone P, Vignolo LA. 1982. Right–left asymmetry in anterior speech region. Arch Neurol 39:239–240.

Flechsig P. 1920. Anatomie des menschlichen Gehirns und Rückenmarks auf myelogenetischer Grundlage. Leipzig: Thieme.

Foundas AL, Leonard CM, Heilman KM. 1995. Morphologic cerebral asymmetries and handedness. Arch Neurol 52:501–508.

Fox PT, Ingham RJ, Ingham JC, Hirsch TB, Downs JH, Martin C, Jerabek P, Glass T, Lancaster JL. 1996. A PET study of the neural systems of stuttering. Nature 382:158–162.

Frackowiak RSJ. 1994. Functional mapping of verbal memory and language. TINS 17:109–115.

Friston KJ. 1996. Statistical parametric mapping and other analysis of functional imaging data. In: Toga AW, Mazziotta JC, editors. Brain mapping. The methods. San Diego: Academic Press. p 363–386.

Galaburda AM. 1980. La region de Broca: observations anatomiques faites un siecle apres la mort de son decoveur. Rev Neurol [Paris] 136:609–616.

Galaburda AM, Geschwind N. 1981. Anatomical asymmetries in the adult and developing brain and their implications for function. Acta Paediatr 28:271–292.

Galaburda AM, Corsiglia J, Rosen GD, Sherman GF. 1987. Planum temporale asymmetry, reappraisal since Geschwind and Levitzky. Neuropsychologia 25:853–868.

Geschwind N, Levitsky W. 1968. Human brain: left–right asymmetries in temporal speech region. Science 130:186–187.

Geyer S, Ledberg A, Schleicher A, Kinomura S, Schormann T, Bürgel U, Klingberg T, Larsson J, Zilles K, Roland PE. 1996. Two different areas within the primary motor cortex of man. Nature 382:805–807.

Geyer S, Schleicher A, Zilles K. 1997. The somatosensory cortex of human: cytoarchitecture and regional distributions of receptor-binding sites. Neuroimage 6:27–45.

Habib M, Gayraud D, Oliva A, Regis J, Salamon G, Khalil R. 1991. Effects of handedness and sex on the morphology of the corpus callosum: a study with brain magnetic resonance imaging. Brain Cogn 16:41–61.

Harasty J, Double KL, Halliday GM, Kril JJ, McRitchie DA. 1997. Language-associated cortical regions are proportionally larger in the female brain. Arch Neurol 54:171–176.

Haug H. 1980. Die Abhängigkeit der Einbettungsschrumpfung des Gehirngewebes vom Lebensalter. Verh Anat Ges 74:699–700.

Hayes TL, Lewis DA. 1995. Anatomical specialization of the anterior motor speech area: hemispheric differences in magnopyramidal neurons. Brain Lang 49:289–308.

Hayes TL, Lewis DA. 1996. Magnopyramidal neurons in the anterior motor speech region. Arch Neurol 153:1277–1283.

Herholz K, Thiel A, Pietrzyk U, Stockhausen HMv, Karbe H, Kessler J, Bruckbauer T, Halber M, Heiss WD. 1996. Individual functional anatomy of verb generation. Neuroimage 3:185–194.

Hertz-Pannier L, Gaillard WD, Mott SH, Cuenod CA, Bookheimer SY, Weinstein S, Conry JPP, Schiff SJ, Le Bihan D, Theodore WH. 1997. Noninvasive assessment of language dominance in children and adolescents with functional MRI: a preliminary study. Neurology 48:1003–1012.

Hier DB, Yoon WB, Mohr JP, Price TR, Wolf PA. 1994. Gender and aphasia in the stroke data bank. Brain Lang 47:155–167.

Hinke RM, Hu X, Stillman AE, Kin SG, Merkle H, Salmi R, Ugurbil K. 1993. Functional magnetic resonance imaging of Broca's area during internal speech. Cogn Neurosci Neuropsychol 4:675–678.

Hirano S, Kojima H, Naito Y, Honjo I, Kamoto Y, Okazawa H, Ishizu K, Yonekura Y, Nagahama Y, Fukuyama H, Konishi J. 1996. Cortical speech processing mechanisms while vocalizing visually presented language. NeuroReport 8:363–367.

Ide A, Rodriguez E, Zaidel E, Aboitiz F. 1996. Bifurcation patterns in the human sylvian fissure: hemispheric and sex differences. Cereb Cortex 6:717–725.

Indefrey P, Gruber O, Brown C, Hagoort P, Posse S, Kleinschmidt A. 1998. Lexicality and not syllable frequency determine lateralized premotor activation during the pronunciation of word-like stimuli—an fMRI study. Neuroimage 7:S4.

Ingvar DH, Schwartz MS. 1974. Blood flow patterns in the dominant hemisphere by speech and reading. Brain 97:273–288.

Jacobs B, Scheibel AB. 1993. A quantitative dendritic analysis of Wernicke's area in humans. I. Lifespan changes. J Comp Neurol 327:83–96.

Jacobs B, Batal HA, Lynch B, Ojemann G, Ojemann LM, Scheibel AB. 1993a. Quantitative dendritic and spine analysis of speech cortices: a case study. Brain Lang 44:239–253.

Jacobs B, Schall M, Scheibel AB. 1993b. A quantitative dendritic analysis of Wernicke's area in humans. II. Gender, hemispheric, and environmental factors. J Comp Neurol 327:97–111.

Jansen Y, Geyer S, Schleicher A, Matelli M, Luppino G, Rizzolatti G, Zilles K. 1996. Receptor autoradiographic and architectonic mapping of the supplementary motor area in the macaque monkey [abstract]. Verh Anat Ges 91:186.

Jäncke L, Schlaug G, Huang Y, Steinmetz H. 1994. Asymmetry of the planum parietale. NeuroReport 5:1161–1163.

Just MA, Carpenter PA, Keller TA, Eddy WF, Thulborn KR. 1996. Brain activation modulated by sentence comprehension. Science 274:114–116.

Kertesz A, Polk M, Black SE, Howell J. 1990. Sex, handedness, and the morphometry of cerebral asymmetries on magnetic resonance imaging. Brain Res 530:40–48.

Kim KHS, Relkin NR, Lee K-M, Hirsch J. 1997. Distinct cortical areas associated with native and second languages. Nature 388:171–174.

Kimura D. 1983. Sex differences in cerebral organization for speech and praxic function. Can J Psychol 37:19–35.

Kononova EP. 1935. Structural variability of the cortex cerebri. Inferior frontal gyrus in adults [in Russian]. In: Sarkisov SA, Filimonoff IN, editors. Annals of the Brain Research Institute. Volume I. Moscow–Leningrad: State Press for Biological and Medical Literature. p 49–118.

Kononova EP. 1938. Variability in the structure of the human cerebral cortex. Frontal lobe of adult man [in Russian]. In: Sarkisov SA, Filimonoff IN, editors. Annals of the Brain Research Institute. Volumes III–IV. Moscow–Leningrad: State Press for Biological and Medical Literature. p 213–274.

Kononova EP. 1949. The frontal lobe [in Russian]. In: Sarkisov SA, Filimonoff IN, Preobrashenskaya NS, editors. The cytoarchitecture of the human cortex cerebri. Moscow: Medgiz. p 309–343.

Kretschmann H-J, Weinrich W. 1996. Dreidimensionale Computergraphik neurofunktionaler Systeme. Stuttgart: Thieme.

Kretschmann H-J, Tafesse U, Herrmann A. 1982. Different volume changes of cerebral cortex and white matter during histological preparation. Microsc Acta 86:13–24.

Levine DN, Mohr JP. 1979. Language after bilateral cerebral infarctions: role of the minor hemisphere in speech. Neurology 29:927–938.

Lieberman P. 1985. On the evolution of human syntactic ability. Its pre-adaptive bases—motor control and speech. J Hum Evol 14:657–668.

Martin NA, Beatty J, Johnson RA, Collaer ML, Vinuela F, Becker DP, Nuwer MR. 1993. Magnetoencephalographic localization of a language processing cortical area adjacent to a cerebral arteriovenous malformation. J Neurosurg 79:584–588.

Mazoyer BM, Tzourio N, Frak V, Syrota A, Murayama N, Levrier O, Salamon G, Dehaene S, Cohen L, Mehler J. 1993. The cortical representation of speech. J Cogn Neurosci 5:467–479.

Mazziotta JC, Metter EJ. 1988. Brain cerebral metabolic mapping of normal and abnormal language and its acquisition during development. Res Publ Assoc Res Nerv Ment Dis 66:245–266.

McCarthy G, Blamire AM, Rothman DL, Gruetter R. 1993. Echo-planar magnetic resonance imaging studies of frontal cortex activation during word generation in humans. Proc Natl Acad Sci USA 90:4952–4956.

McGlone J. 1977. Sex differences in the cerebral organization of verbal functions in patients with unilateral brain lesions. Brain 100:775–793.

McGlone J. 1980. Sex differences in human brain asymmetry: a critical survey. Behav Brain Sci 3:215–263.

Merker B. 1983. Silver staining of cell bodies by means of physical development. J Neurosci 9:235–241.

Mohr JP. 1973. Rapid amelioration of motor aphasia. Arch Neurol 28:77–82.

Mohr JP, Pessin MS, Finkelstein S, Funkenstein HH, Duncan GW, Davis KR. 1978. Broca aphasia: pathologic and clinical. Neurology 28:311–324.

Nathaniel-James DA, Fletcher P, Frith CD. 1997. The functional anatomy of verbal initiation and suppression using the Hayling test. Neuropsychologia 35:559–566.

Nichelli P, Grafman J, Pietrini P, Clark K, Lee KY, Miletich R. 1995. Where the brain appreciates the moral of a story. NeuroReport 6:2309–2313.

Ojeman GA. 1991. Cortical organization of language. J Neurosci 11:2281–2287.

Ono M, Kubik S, Abernathey CD. 1990. Atlas of the cerebral sulci. New York: Thieme.

Paulesu E, Frith U, Snowling M, Gallagher A, Morton J, Frackowiak RSJ, Frith CD. 1996. Is developmental dyslexia a disconnection syndrome? Evidence from PET scanning. Brain 119:143–157.

Pedersen PM, Jorgensen HS, Nakayama H, Raauschou HO, Olsen TS. 1995. Aphasia in acute stroke: incidence, determinants, and recovery. Ann Neurol 38:659–666.

Penfield W, Rasmussen T. 1949. Vocalization and arrest of speech. Arch Neurol Psychiatry 61:21–27.

Penhune VB, Zatorre RJ, MacDonald JD, Evans AC. 1996. Interhemispheric anatomical differences in human primary auditory cortex: probabilistic mapping and volume measurement from magnetic resonance scans. Cereb Cortex 6:661–672.

Petersen SE, Fox PT, Posner MM, Raichle ME. 1988. Positron emission tomographic studies of the cortical anatomy of single word processing. Nature 331:585–589.

Petrides M, Pandya DN. 1994. Comparative architectonic analysis of the human and the macaque frontal cortex. In: Boller F, Grafman J, editors. Handbook of neuropsychology. New York: Elsevier. p 17–58.

Petrides M, Alivisatos B, Meyer E, Evans AC. 1993. Functional activation of the human frontal cortex during the performance of verbal working memory tasks. Proc Natl Acad Sci USA 90:878–882.

Pfeifer R. 1920. Myelogenetisch-anatomische Untersuchungen über das kortikale Ende der Hörleitung. Abhandl Math Phys Klein Sächs Akad Wissenschaft 37:1–54.

Poeppel D. 1996a. A critical review of PET studies of phonological processing. Brain Lang 55:317–351.

Poeppel D. 1996b. Some remaining questions about studying phonological processing with PET: response to Demonet, Fiez, Paulesu, Petersen, and Zatorre. Brain Lang 55:380–385.

Preuss TM, Goldman-Rakic PS. 1991. Myelo- and cytoarchitecture of the granular frontal cortex and surrounding regions in the stresirhine primate *Galago* and the anthropoid primate *Macaca*. J Comp Neurol 310:429–474.

Rabinowicz T. 1967. Quantitative appraisal of the cerebral cortex of the premature infant of 8 months. In: Minkowsky AA, editor. Regional development of the brain in early life. Oxford: Blackwell Scientific Publications. p 92–118.

Rademacher J, Caviness J, Steinmetz H, Galaburda AM. 1993. Topographical variation of the human primary cortices: implications for neuroimaging, brain mapping, and neurobiology. Cereb Cortex 3:313–329.

Rajkowska G, Goldman-Rakic PS. 1995a. Cytoarchitectonic definition of prefrontal areas in the normal human cortex: I. Remapping of areas 9 and 46 using quantitative criteria. Cereb Cortex 5:307–322.

Rajkowska G, Goldman-Rakic PS. 1995b. Cytoarchitectonic definition of prefrontal areas in the normal human cortex: II. Variability in locations of areas 9 and 46 and relationship to the Talairach coordinate system. Cereb Cortex 5:323–337.

Riegele L. 1931. Die Cytoarchitektonik der Felder der Broca'schen Region. J Psychol Neurol 42:496–514.

Rizzolatti G, Arbib MA. 1998. Language within our grasp. Trends Neurosci 21:188–194.

Roland PE. 1993. Brain activation. New York: Wiley-Liss.

Roland PE, Zilles K. 1994. Brain atlases—a new research tool. Trends Neurosci 17:458–467.

Roland PE, Zilles K. 1996. The developing European computerized human brain database for all imaging modalities. Neuroimage 4:S39–S47.

Roland PE, Zilles K. 1998. Structural divisions and functional fields in the human cerebral cortex. Brain Res Rev 26:87–105.

Roland PE, Friberg L, Lassen NA, Olsen TS. 1985. Regional cortical blood flow changes during production of fluent speech and during conservation. J Cereb Blood Flow Metab 5:S205–S206.

Sanides F. 1975. Comparative neurology of the temporal lobe in primates including man with reference to speech. Brain Lang 2:396–419.

Sarkisov SA, Filimonoff IN, Preobrashenskaya NS. 1949. Cytoarchitecture of the human cortex cerebri [in Russian]. Moscow: Medgiz.

Scheibel AB. 1984. A dendritic correlate of human speech. In: Geschwind N, Galaburda AM, editors. Cerebral dominance. Cambridge: Harvard University Press. p 43–52.

Scheibel AB, Paul LA, Fried I, Forsythe AB, Tomiyasu U, Wechsler A, Kao A, Slotnick J. 1985. Dendritic organization of the anterior speech area. Exp Neurol 87:109–117.

Schlaepfer TE, Harris GJ, Tien AY, Peng L, Lee S, Pearlson GD. 1995. Structural differences in the cerebral cortex of healthy female and male subjects: a magnetic resonance imaging study. Psychiatr Res Neuroimag 61:129–135.

Schlaug G, Jäncke L, Huang Y, Steinmetz H. 1995a. In vivo evidence of structural brain asymmetry in musicians. Science 267:699–701.

Schlaug G, Schleicher A, Zilles K. 1995b. Quantitative analysis of the columnar arrangement of neurons in the human cingulate cortex. J Comp Neurol 351:441–452.

Schleicher A, Zilles K. 1990. A quantitative approach to cytoarchitectonics: analysis of structural inhomogeneities in nervous tissue using an image analyser. J Microsc 157:367–381.

Schleicher A, Amunts K, Geyer S, Simon U, Zilles K, Roland PE. 1995. A method of observer-independent cytoarchitectonic mapping of the human cortex. Human Brain Mapping 1(Suppl):77.

Schleicher A, Amunts K, Geyer S, Morosan P, Zilles K. 1998. Observer-independent method for microstructural parcellation of cerebral cortex: a quantitative approach to cytoarchitectonics. Neuroimage 9:165–177.

Schormann T, Zilles K. 1997. Limitations of the principle axes theory. IEEE Trans Med Imaging 16:942–947.

Schormann T, Zilles K. 1998. Three-dimensional linear and nonlinear transformations: an integration of light microscopical and MRI data. HBM 6:339–347.

Schormann T, Matthey Mv, Dabringhaus A, Zilles K. 1993. Alignment of 3-D brain data sets originating from MR and histology. Bioimaging 1:119–128.

Schormann T, Dabringhaus A, Zilles K. 1995. Statistics of deformations in histology and improved alignment with MRI. IEEE Trans Med Imaging 14:25–35.

Sergent J, Zuck E, Levesque M, MacDonald B. 1992. Positron emission tomography study of letter and object processing: empirical findings and methodological considerations. Cereb Cortex 2:68–80.

Shaywitz BA, Shaywitz SE, Pugh KR, Constable RT, Skudlarski P, Fulbright RK, Bronen RA, Fletcher JM, Shankweliler DP, Katz L, Gore JC. 1995. Sex differences in the functional organization of the brain for language. Nature 373:607–609.

Simonds RJ, Scheibel AB. 1989. The postnatal development of the motor speech area: a preliminary study. Brain Lang 37:43–58.

Skullerud K. 1985. Variations in the size of the human brain. Acta Neurol Scand 71:1–94.

Steinmetz H. 1996. Structure, function and cerebral asymmetry: in vivo morphometry of the planum temporale. Neurosci Biobehav Rev 29:587–591.

Steinmetz H, Rademacher J, Jäncke L, Huan Y, Thron A, Zilles K. 1990. Total surface of temporoparietal intrasylvian cortex: diverging left–right asymmetries. Brain Lang 39:357–372.

Steinmetz H, Volkmann J, Jäncke L, Freund HJ. 1991. Anatomical left–right asymmetry of language-related temporal cortex is different in left and right handers. Ann Neurol 29:315–319.

Steinmetz H, Staiger JF, Schlaug G, Huang Y, Jäncke L. 1995. Corpus callosum and brain volume in women and men. NeuroReport 6:1002–1004.

Stengel E. 1930. Morphologische und cytoarchitektonische Studien über den Bau der unteren Frontalwindung bei Normalen und Taubstummen. Ihre individuellen und Seitenunterschiede. Z Exp Angew Psychol 130:630–677.

Strasburger EH. 1938. Vergleichende myeloarchitektonische Studien an der erweiterten Brocaschen Region des Menschen. J Psychol Neurol 48:477–511.

Talairach J, Tournoux P. 1988. Coplanar stereotaxic atlas of the human brain. Stuttgart: Thieme.

Uylings HBM, Eden CGv, Verwer RWH. 1984. Morphometric methods in sexual dimorphism research on the central nervous system. In: DeVries GD, editor. Progress in brain research. Amsterdam: Elsevier. p 215–222.

Uylings HBM, Eden GCv, Hofman MA. 1986. Morphometry of size/volume variables and comparison of their bivariate relations in the nervous system under different conditions. J Neurosci Methods 18:19–37.

Uylings HBM, Malofeeva LI, Bogolepova IN, Amunts K, Zilles K. 1999. Broca's language area from a neuroanatomical and developmental perspective. In: Hagoort P, Brown C, editors. Neurocognition of language processing. Oxford: Oxford University Press. Forthcoming.

Vierordt H. 1893. Anatomische, physiologische und physikalische Daten und Tabellen zum Gebrauch für Mediziner. Jena: Fischer Verlag.

Vogt O. 1910. Die myeloarchitektonische Felderung des menschlichen Stirnhirns. J Psychol Neurol 15:221–238.

Vogt C, Vogt O. 1919. Allgemeinere Ergebnisse unserer Hirnforschung. J Psychol Neurol 25:292–398.

Witelson SF, Kigar DL. 1992. Sylvian fissure morphology and asymmetry in men and women: bilateral differences in relation to handedness in men. J Comp Neurol 323:326–340.

Witelson SF, Pallie W. 1973. Left hemisphere specialization for language in the newborn. Neuroanatomical evidence of asymmetry. Brain 96:641–646.

Wree A, Schleicher A, Zilles K. 1982. Estimation of volume fractions in nervous tissue with an image analyzer. J Neurosci Methods 6:29–43.

Zatorre RJ, Evans AC, Meyer E, Gjedde A. 1992. Lateralization of phonetic and pitch discrimination in speech processing. Science 256:846–849.

Zatorre RJ, Meyer E, Gjedde A, Evans AC. 1996. PET studies of phonetic processing of speech: review, replication, and reanalysis. Cereb Cortex 6:21–30.

Zilles K, Armstrong E, Schlaug G, Schleicher A. 1986a. Quantitative cytoarchitectonics of the posterior cingulate cortex in primates. J Comp Neurol 253:514–524.

Zilles K, Werners R, Büsching U, Schleicher A. 1986b. Ontogenesis of the laminar structures in area 17 and 18 of the human visual cortex. A quantitative study. Anat Embryol 174:129–144.

Zilles K, Armstrong E, Schleicher A, Kretschmann H-J. 1988. The human pattern of gyrification in the cerebral cortex. Anat Embryol 179:173–179.

Zilles K, Schlaug G, Matelli M, Luppino G, Schleicher A, Qü M, Dabringhaus A, Seitz R, Roland PE. 1995. Mapping of human and macaque sensorimotor areas by integrating architectonic, transmitter receptor, MRI and PET data. J Anat 187:515–537.